The Reductive Chemistry of Nickel Hydroporphyrins. Evidence for a Biologically Significant Difference between Porphyrins, Hydroporphyrins, and Other Tetrapyrroles

Alan M. Stolzenberg* and Matthew T. Stershic

Contribution from the Department of Chemistry, Brandeis University, Waltham, Massachusetts 02254. *Received July 2, 1987*

Abstract: The chemical and electrochemical reductions of nickel porphyrin and hydroporphyrin complexes in the octaethyl, tetraphenyl, and methylated octaethyl series were investigated in nonaqueous media. The potentials for reduction of the complexes were determined by cyclic voltammetry in three solvents. A single, reversible, one-electron reduction was observed near −1.5 V versus SCE for most complexes in acetonitrile and dimethylformamide. Ni(OEiBC) and Ni(DMOEiBC) had voltammograms with shapes characteristic of electrocatalytic processes when reduced in methylene chloride. Other complexes were generally reduced irreversibly ($i_{p,a} < i_{p,c}$) in this solvent. UV–vis, EPR, and ^{1}H NMR spectroscopy were used to characterize the reduced species obtained by electrochemical and chemical means. The site of reduction depends upon the method of reduction (and the time scale of the method), the saturation level of the macrocycle, and the identity of the substituents on the macrocycle. Ni(OEP) is reduced to the anion radical Ni(OEP)$^{\bullet-}$, which undergoes further reduction to afford the stable, diamagnetic phlorin anion complex Ni(OEPH)$^-$. Ni(OEC) and Ni(DMOEiBC) are reduced to transient nickel(I) complexes. Ni^{I}(OEC)$^-$ reacts further to give the chlorin–phlorin anion complex Ni(OECH)$^-$. Ni(OEiBC) is reduced to Ni^{I}(OEiBC)$^-$. Aside from reduced F_{430}, Ni^{I}(OEiBC)$^-$ is the first stable nickel(**I**) tetrapyrrole and is the only known nickel(I) complex that has a π-system extending over the entire macrocycle. Chemical reductions of Ni(TPP), Ni(TPC), and Ni(TPiBC) produce mixtures of anion radical, phlorin anion, and phlorin dianion species. The macrocycles that appear best able to accommodate the large, approximately 2.1 Å Ni–N distance required by nickel(I) are those that were shown to ruffle in neutral, low-spin nickel(II) complexes. One consequence of ruffling is a reduction in the macrocycle core size to give smaller Ni–N distances (1.92 Å) than typically observed in a porphyrin environment. Apparently, the hole size/ligand field strength of hydroporphyrins can be varied over a wide range at little cost in energy. Further consideration of the conformational energy of these complexes suggests that a fundamental difference between porphyrins, hydroporphyrins, corrins, oxoporphyrins, and other tetrapyrrole macrocycles is their optimal hole size and the range of hole sizes that are readily accessible in their complexes. The effects of the stereochemistry of the macrocycle substituents are discussed, and an explanation is developed for the widely varying affinities of nickel tetrapyrroles for axial ligands.

Factor F_{430} is the only known nickel-containing tetrapyrrole of biological significance. It is a prosthetic group of methyl-coenzyme M reductase,[1] an enzyme which catalyzes the reductive cleavage of *S*-methyl coenzyme M (2-(methylthio)ethanesulfonate) to methane.[2] The extensively saturated hydroporphyrin[3] macrocycle of F_{430} is an example of the tetrahydrocorphin ring system.[4]

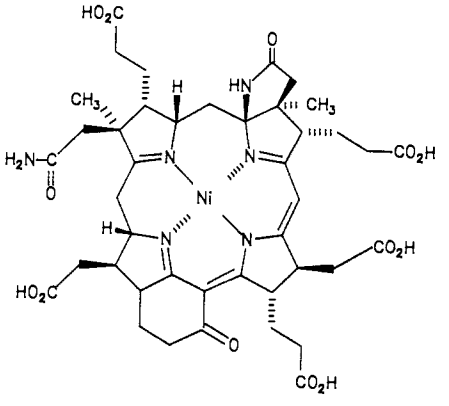

F_{430}

Despite great interest, a question that remains unanswered is why modified tetrapyrroles ligands like those found in F_{430}, siroheme, and vitamin B_{12} are employed to carry out selected chemistries rather than a porphyrin ligand. Several lines of evidence suggest that these modified tetrapyrrole ligands are more flexible than porphyrins.[5-10] Studies of the conformations of nickel hydroporphyrin complexes, both in solution[5,11] and in the solid state,[6-9,12] have been particularly revealing. To date, however, no significant and biologically-relevant change in metal-based reactivity has been demonstrated to occur upon substitution of one class of macrocycle for another.

Recently, an EPR signal was detected in whole cells of *Methanobacterium thermoautotrophicum* and was attributed to F_{430} in intact, active enzyme.[13] The *g* values and hyperfine coupling associated with this signal were consistent with a d^9-Ni(I) ion coordinated by four nitrogen atoms.[14] Examples of nickel(I) complexes with nitrogen donor ligands are relatively few in number[14-19] and are mainly restricted to tetraaza macrocyclic

(1) Ellefson, W. L.; Whitman, W. B.; Wolfe, R. S. *Proc. Natl. Acad. Sci. U.S.A.* **1982**, *79*, 3707.
(2) Ellefson, W. L.; Wolfe, R. S. *J. Biol. Chem.* **1980**, *255*, 8388. Nagle, D. P.; Wolfe, R. S. *Proc. Natl. Acad. Sci. U.S.A.* **1983**, *80*, 2151.
(3) (a) Scheer, H. In *The Porphyrins*; Dolphin, D., Ed.; Academic: New York, 1978; Vol. 2, pp 1–44. (b) Scheer, H.; Inhoffen, H. H. *Ibid.* pp 45–90.
(4) (a) Pfalz, A.; Jaun, B.; Fässler, A.; Eschenmoser, A.; Jaenchen, R.; Gilles, H. H.; Diekert, G.; Thauer, R. K. *Helv. Chim. Acta* **1982**, *65*, 828. (b) Livingston, D. A.; Pfaltz, A.; Schreiber, J.; Eschenmoser, A.; Ankel-Fuchs, D.; Moll, J.; Jaenchen, R.; Thauer, R. K. *Helv. Chim. Acta* **1984**, *67*, 334. (c) Pfaltz, A.; Livingston, D. A.; Jaun, B.; Diekert, G.; Thauer, R. K.; Eschenmoser, A. *Helv. Chim. Acta* **1985**, *68*, 1338. (d) Fässler, A.; Kobelt, A.; Pfaltz, A.; Eschenmoser, A.; Bladon, C.; Battersby, A. R.; Thauer, R. K. *Helv. Chim. Acta* **1985**, *68*, 2287.
(5) Stolzenberg, A. M.; Stershic, M. T. *Inorg. Chem.* **1987**, *26*, 1970.
(6) Strauss, S. H.; Silver, M. E.; Ibers, J. A. *J. Am. Chem. Soc.* **1983**, *105*, 4108.
(7) Strauss, S. H.; Silver, M. E.; Long, K. M.; Thompson, R. G.; Hudgens, R. A.; Spartalian, K.; Ibers, J. A. *J. Am. Chem. Soc.* **1985**, *107*, 4207.
(8) (a) Suh, M. P.; Swepston, P. N.; Ibers, J. A. *J. Am. Chem. Soc.* **1984**, *106*, 5164. (b) Gallucci, J. C.; Swepston, P. N.; Ibers, J. A. *Acta Crystallogr., Sect. B: Struct. Crystallogr. Cryst. Chem.* **1982**, *B38*, 2134.
(9) Kratky, C.; Waditshatka, R.; Angst, C.; Johansen, J. E.; Plaquevent, J. C.; Schreiber, J.; Eschenmoser, A. *Helv. Chim. Acta* **1985**, *68*, 1312.
(10) Geno, M. K.; Halpern, J. *J. Am. Chem. Soc.* **1987**, *109*, 1238.
(11) Waditschatka, R.; Kratky, C.; Jaun, B.; Heinzer, J.; Eschenmoser, A. *J. Chem. Soc., Chem. Commun.* **1985**, *1604*.
(12) Kratky, C.; Angst, C.; Johansen, J. E. *Angew. Chem., Int. Ed. Engl.* **1981**, *20*, 211.
(13) Albract, S. P. J.; Ankel-Fuchs, D.; Van der Zwaan, J. W.; Fontjin, R. D.; Thauer, R. K. *Biochim. Biophys. Acta* **1986**, *870*, 50.
(14) Lovecchio, F. V.; Gore, E. S.; Busch, D. H. *J. Am. Chem. Soc.* **1974**, *96*, 3109.
(15) Nag, K.; Chakravorty, A. *Coord. Chem. Rev.* **1980**, *33*, 87.
(16) (a) Gagne, R. R.; Ingle, D. M. *J. Am. Chem. Soc.* **1980**, *102*, 1444. (b) Gagne, R. R.; Ingle, D. M. *Inorg. Chem.* **1981**, *20*, 420.

0002-7863/88/1510-6391$01.50/0

ligands that lack a conjugated α-imine group.[14,16a] The only cases known where the ligand contains this functionality are the Ni(I) forms of free F_{430} and of F_{430} pentamethyl ester.[20,21] These are also the only known examples of Ni(I) tetrapyrrole complexes.

The reductive chemistry of nickel porphyrin complexes has received little attention compared with the extensive investigations of Co, Fe, and Mn porphrins.[22,23] Nickel hydroporphyrin complexes remain virtually uninvestigated.[24] Generally, reduction of a Ni(II) porphyrin is assumed to result in formation of the porphyrin anion radical.[22,24] With the exception of Ni(TPP),[25] no second reduction to yield a dianion has been reported. This is surprising and inexplicable. Given the normal potential difference between first and second reductions of porphyrins,[22,23] the second reductions of nickel porphyrin complexes should fall well within the range of accessible potentials. This situation has been remarked upon[22] but has not elicited further investigation.

Our interest in the chemistry of nickel hydroporphyrins[5] and of F_{430} has led us to undertake a systematic investigation of the chemistry of reduced nickel porphyrin and hydroporphyrin complexes. In this paper, we describe the preparation and characterization of the reduced nickel complexes. The results establish that important and substantive differences exist in the flexibility and ligand fields/hole sizes of hydroporphyrins and porphyrins. These differences affect and distinguish the metal-based reactivities of metalloporphyrins and -hydroporphyrins. The level of saturation of the macrocycle π-system and the identity of macrocycle substituents strongly affect the chemistry of the reduced complexes. We report the synthesis of the Ni(I) octaethylisobacteriochlorin anion, $Ni^{I}(OEiBC^{26})^{-}$, the first stable Ni(I) tetrapyrrole complex with a π-system extending over the macrocycle. $Ni^{I}(OEiBC)^{-}$ shows considerable promise in modeling the reactions of F_{430}-dependent methanogenesis. It reacts rapidly, in both a stoichiometric and a catalytic manner, with alkyl halides and other alkylating reagents to give the corresponding alkane. Details of the reactions of reduced nickel complexes are presented in a companion paper.[27] A brief account of a portion of this work has appeared previously.[28]

Experimental Section

General Comments. All manipulations were carried out under a nitrogen or argon atmosphere by use of Schlenk techniques or in a Vacuum/Atmospheres Co. drybox. 2-MeTHF was dried by distillation from sodium benzophenone ketyl. Other reagents and solvents were treated as previously reported and were thoroughly degassed prior to use.[29]

EPR spectra were determined on a Varian E-6 spectrometer. Unless otherwise noted, spectra were of frozen samples at about 100 K. Absorption spectra were recorded on a Perkin-Elmer Lambda 4C spectrophotometer. Spectra of electrochemically reduced species were obtained with an optically transparent thin-layer electrode cell (OTTLE). The OTTLE was of a gold minigrid (200 lines/in)-quartz microscope slide variety and has been described previously.[30] A miniature sodium chloride saturated calomel electrode (−7 mV versus SCE) was employed as the reference electrode for OTTLE experiments. The OTTLE cell was loaded in an inert atmosphere drybox immediately prior to its use. Bulk electrolyses were attempted inside the drybox in an H-cell of roughly 30-mL capacity. The three electrode compartments were separated by fritted glass or porous vycor disks. Potentials are reported relative to the SCE reference electrode. Other spectroscopic and electrochemical measurements were obtained as before.[29]

Preparation of Complexes. Ni(OEP),[31] *trans*-Ni(OEC)[5] (hereafter referred to as simply Ni(OEC)), H_2(OEiBC),[30] Ni(TPP),[32] H_2(TPC),[33] and H_2(TPiBC)[33] were prepared by literature methods. In our hands, the phosphoric acid extraction procedures reported in the workup of H_2(TPC) and H_2(TPiBC) were not beneficial and were omitted. As obtained, H_2(TPiBC) was always contaminated by small but detectable H_2(TPBC) and H_2(TPC) impurities which were not removed by recrystallization, chromatography, extractions, or other methods. H_2(MOEC) and H_2(DMOEiBC) were prepared[34] from the respective oxoporphyrins 3,3,7,8,12,13,17,18-octaethyl-2-porphinone[29] and 3,3,8,8,12,13,17,18-octaethyl-2,7-porphindione.[29] The quantity of the MOEC and DMOEiBC compounds that was available was extremely limited (insufficient to permit analyses) owing to the difficulty of access to oxoporphyrin starting materials and the low yields of the synthetic procedures.

Ni(OEiBC). A 100-mg sample of H_2(OEiBC), which is a 1:1 mixture of *tct* and *ttt* diastereoisomers, was dissolved in 50 mL of absolute ethanol and was placed under a nitrogen atmosphere. $Ni(OAc)_2 \cdot 4H_2O$ (200 mg) was added, and the resulting mixture was heated at reflux. The progress of the metalation reaction was monitored by UV–vis spectroscopy. When the reaction was complete, the ethanol was removed under vacuum to afford the product as a blue residue. The product was purified by chromatography on silica gel. Elution was with a 140:20:3.2 mixture of hexane/benzene/triethylamine. Evaporation of the eluate gave a blue-purple solid which was recrystallized from diethyl ether/methanol. Purple crystals were obtained in yields above 90%. Characterization data reported for *tct*-Ni(OEiBC)[35] agreed with the data that we obtained in the same solvents: UV–vis (CH_3CN) λ_{max}, nm (10^{-3} ϵ_M, cm^{-1}) 345 (sh, 23.1), 371 (sh, 51.4), 381 (56.0), 517 (6.4), 547 (11.0), 592 (55.5); UV–vis (THF) λ_{max}, nm (10^{-3} ϵ_M, cm^{-1}) 385 (56.0), 524 (8.2), 548 (12.6), 592 (54.4).

Ni(MOEC). A solution of 25 mg of H_2(MOEC) and 40 mg of $NiCl_2 \cdot 6H_2O$ in 20 mL of DMF was refluxed under nitrogen for 2 h. After the blue solution cooled to room temperature, 50 mL of water was added. The product precipitated. The mixture was extracted with several portions of chloroform. The combined extracts were evaporated to dryness. The crude product was purified by chromatography on grade III neutral alumina. Elution was with benzene. The product was recrystallized from chloroform/methanol: UV–vis (C_6H_6) λ_{max}, nm (A_λ/A_{618}) 399 (2.05), 491 (0.13), 524(0.11), 577 (0.18), 618 (1.00); ^{1}H NMR ($CDCl_3$) δ 0.63, 1.03 (t, 3 H each, pyrroline CH_3), 1.55–1.8 (m, pyrrole CH_3), 1.62 (d, β-CH_3), 1.8–2.05 (m, 3 H, A and B and A′ portions of ABX_3 and A′B′X$_3$′ multiplets, pyrroline CH_2), 2.42 (m, 1 H, B′ portion of A′B′X$_3$′ multiplet, pyrroline CH_2), 3.51 (q, pyrrole CH_2), 3.62 (m, pyrrole CH_2), 4.32 (q, 1 H, β-H), 7.91, 8.04, 9.05, 9.07 (s, 1 H each, meso-H).

Ni(DMOEiBC). This complex was prepared from H_2(DMOEiBC) by the same method used to prepare Ni(OEiBC). The complex is a mixture (approximately 1:1) of two diastereomers: 2,7-dimethyl syn and 2,7-dimethyl anti. This is reflected in the ^{1}H NMR (below) by the

(17) Becker, J. Y.; Kerr, J. B.; Pletcher, D.; Rosas, R. *J. Electroanal. Chem.* **1981**, *117*, 87.

(18) (a) Ansell, C. W. G.; Lewis, J.; Raithby, P. R.; Ramsden, J. N.; Schröder, M. *J. Chem. Soc., Chem. Commun.* **1982**, *546*. (b) Constable, E. C.; Lewis, J.; Schröder, M. *Polyhedron* **1982**, *1*, 311. (c) Constable, E. C.; Lewis, J.; Liptrot, M. C.; Raithby, P. R.; Schröder, M. *Polyhedron* **1983**, *2*, 301.

(19) Dietrich-Buchecker, C. O.; Kern, J.-M.; Sauvage, J.-P. *J. Chem. Soc., Chem. Commun.* **1985**, 760.

(20) Jaun, B.; Pfaltz, A. *J. Chem. Soc., Chem. Commun.* **1986**, 1327.

(21) This statement excludes the special cases of pentadentate macrocycles, which are incapable of forming low-spin Ni(II) complexes. See ref 18a and 18c.

(22) Kadish, K. M. *Prog. Inorg. Chem.* **1986**, *34*, 525.

(23) (a) Felton, R. H. In *The Porphyrins*; Dolphin, D., Ed.; Academic: New York, 1978; Vol. 5, pp 53–125. (b) Fuhrhop, J.-H.; Kadish, K. M.; Davis, D. G. *J. Am. Chem. Soc.* **1973**, *95*, 5140.

(24) Chang, D.; Malinski, T.; Ulman, A.; Kadish, K. M. *Inorg. Chem.* **1984**, *23*, 817.

(25) Felton, R. H.; Linschitz, H. *J. Am. Chem. Soc.* **1966**, *88*, 1113.

(26) Abbreviations: OEP, 2,3,7,8,12,13,17,18-octaethylporphyrin dianion; OEC, 2,3-dihydro-2,3,7,8,12,13,17,18-octaethylporphyrin dianion (chlorin); OEiBC, mixture of *ttt*- and *tct*-2,3,7,8-tetrahydro-2,3,7,8,12,13,17,18-octaethylporphyrin dianion (isobacteriochlorin); OEPH, 5-hydro-2,3,7,8,12,13,17,18-octaethylporphyrin trianion (phlorin); OECH, 2,3,10-trihydro-2,3,7,8,12,13,17,18-octaethylporphyrin trianion (β-chlorin phlorin, see text); MOEC, 2-hydro-2-methyl-3,3,7,8,12,13,17,18-octaethylporphyrin dianion; DMOEiBC, mixture of *syn*- and *anti*-2,7-dihydro-2,7-dimethyl-3,3,8,8,12,13,17,18-octaethylporphyrin dianion; TPP, 5,10,15,20-tetraphenylporphyrin dianion; TPC, 2,3-dihydro-5,10,15,20-tetraphenylporphyrin dianion; TPBC, 2,3,12,13-tetrahydro-5,10,15,20-tetraphenylporphyrin dianion; TPiBC, 2,3,7,8-tetrahydro-5,10,15,20-tetraphenylporphyrin dianion; $OEPMe_2$, 5,15-dihydro-5,15 dimethyl-2,3,7,8,12,13,17,18-octaethylporphyrin dianion, DMF, *N*,*N*-dimethylformamide; THF, tetrahydrofuran; 2-MeTHF, 2-methyltetrahydrofuran; TEAP, tetraethylammonium perchlorate; TBAP, tetra-*n*-butylammonium perchlorate.

(27) Stolzenberg, A. M.; Stershic, M. T. *J. Am. Chem. Soc.* **1988**, *110*, 5397.

(28) Stolzenberg, A. M.; Stershic, M. T. *Inorg. Chem.* **1987**, *26*, 3082.

(29) Stolzenberg, A. M.; Glazer, P. A.; Foxman, B. M. *Inorg. Chem.* **1986**, *25*, 983.

(30) Stolzenberg, A. M.; Spreer, L. O.; Holm, R. H. *J. Am. Chem. Soc.* **1980**, *102*, 364.

(31) Falk, J. E. *Porphyrins and Metalloporphyrins*; Elsevier: New York, 1964.

(32) *Inorganic Synthesis*; Busch, D. H., Ed.; Wiley: New York, 1980; Vol. 20, p 143.

(33) Whitlock, H. W., Jr.; Hanauer, R.; Oster, M. Y.; Bower, B. K. *J. Am. Chem. Soc.* **1969**, *91*, 7485.

(34) Chang, C. K. *Biochemistry* **1980**, *19*, 1971.

(35) Johansen, J. E.; Angst, C.; Kratky, C.; Eschenmoser, A. *Angew. Chem., Int. Ed. Engl.* **1980**, *19*, 141.

presence of two closely spaced peaks for three of the meso positions and by the two different β proton environments and couplings: UV-vis (C_6H_6) λ_{max}, nm (A_λ/A_{593}) 388 (1.01), 549 (0.23), 593 (1.00); UV-vis (C_5H_5N) λ_{max}, nm (A_λ/A_{595}) 396 (1.18), 550 (0.23), 595 (1.00); ^{1}H NMR ($CDCl_3$) δ 0.45, 0.50, 0.59, 0.71, 0.87, 0.92, 1.03, 1.07 (t, pyrroline CH_3), 1.3–1.6 (m, pyrrole CH_3 and β-CH_3), 1.6–2.3 (m, pyrroline CH_2), 3.08–3.32 (m, pyrrole CH_2), 3.55 (q, β-H), 3.75 (m, β-H), [6.35, 6.40], [7.03, 7.08], [7.16, 7.18], 8.29 (s, 1 H each, meso-H).

Ni(TPC). Like H_2(TPP),[32] metalation of H_2(TPC) with nickel cannot be driven to completion. A solution of 50 mg of H_2(TPC) and 100 mg of $NiCl_2 \cdot 6H_2O$ in 30 mL of DMF was refluxed under nitrogen for 4 h. Longer reaction times did not increase the extent of metalation. The solution was cooled to room temperature, and 50 mL of water was added. The product was extracted with several portions of chloroform. The combined extracts were evaporated to dryness, and the residue was recrystallized from hot toluene. Small but detectable levels (by ^{1}H NMR) of H_2(TPC) and H_2(TPP) were present in the crystalline product: UV-vis (C_6H_6) λ_{max} nm (A_λ/A_{617}) 417 (6.29), 617 (1.00); ^{1}H NMR ($CDCl_3$) δ 3.77 (s, 4 H, pyrroline β-H), 7.1–7.9 (m, phenyls), 7.96, 8.27 (d, J = 5 Hz, 2 H each, pyrrole β-H), 8.11 (s, 2 H, pyrrole β-H).

Ni(TPiBC). A solution of 50 mg of H_2(TPiBC) and 100 mg of $NiCl_2 \cdot 6H_2O$ in 30 mL of DMF was refluxed under nitrogen for 4 h (until the UV-vis spectrum showed that metalation was complete). The solution was cooled to room temperature, and 50 mL of water was added. The product was extracted with several portions of chloroform. The combined extracts were evaporated to dryness, and the residue was purified by chromatography on silica gel. Elution was with 40/60 benzene/hexane. The product contained small but detectable levels of H_2(TPBC) (band at 742 nm) and presumably Ni(TPBC) (broad band at 775 nm). Further attempts at purification did not remove these impurities, but instead led to the appearance of shoulders at 640 and 350 nm in the UV-vis spectrum, suggesting partial degradation (oxidation?) of the product: UV-vis (C_6H_6) λ_{max} nm (A_λ/A_{594}) 401 (1.81), 411 (1.83), 520 (0.18), 550 (0.29), 594 (1.00); ^{1}H NMR ($CDCl_3$) δ 3.22 (s, pyrroline β-H), 7.1–7.7 (m, pyrrole β-H and phenyl-H).

Amalgam Reductions. Reductions with sodium amalgam (0.5–1.0%) were carried out in acetonitrile or THF solution. Reactions were prepared and generally carried out inside the drybox. Dilute solutions were used to ensure that the less soluble neutral starting complexes were completely dissolved. At the scale of the experiments, oxidizing impurities and trace water in dried solvents can be present in near stoichiometric quantities. Solvents were pretreated with an aliquot of amalgam prior to use in experiments. Even then, excess amalgam was required to effect complete reduction of the complexes. In a typical preparative experiment, 5 mg of complex was dissolved in 25 mL of solvent and was reacted with excess amalgam (about 100 equiv). The solution and amalgam were constantly stirred. Aliquots were removed periodically to monitor the progress of the reaction by UV-vis spectroscopy. Reduction was complete in 1–2 h. At the desired point in the reaction, the solution was decanted from the amalgam and was reduced to the proper volume for the experiment of interest. Experiments to more accurately follow the progress of the reductions were carried out in tightly-stoppered 1-cm cuvettes equipped with miniature magnetic stir bars. Dilute solutions were reduced in situ in the cuvettes.

1. Ni(OEPH)$^-$. Ni(OEP) was reduced in protio-THF as described above. When the reduction was complete, the solvent was removed in vacuo without heating. The residue was redissolved in CD_3CN that had been pretreated with sodium amalgam. ^{1}H NMR (CD_3CN) δ 7.22 (s, 2 H, 10,20-meso H), 6.70 (s, 1 H, 15 meso-H), 3.03 (s, 2 H, 5 meso CH_2), 2.8–3.0 (m, ethyl CH_2), 1.2–1.4 (m, ethyl CH_3). The spectrum also had peaks attributable to THF, which presumably solvates the sodium counterion.

2. Ni(OECH)$^-$. The complex was prepared as for Ni(OEPH)$^-$: ^{1}H NMR (CD_3CN) δ 6.94 (s, 1 H, 15-meso H), 5.92, 5.87 (s, 1 H each, 5,20-meso H), 2.55–2.82 (m, pyrrole ethyl CH_2 and saturated meso CH_2), 1.5–1.7 (m, pyrroline β-H), 1.25–1.4 (m, pyrroline CH_2), 1.05–1.25 (m, pyrrole CH_3), 1.03, 0.90 (t, 3 H each, pyrroline CH_3).

Results

Voltammetry. Cyclic voltammetry was used to examine the reductions of free-base and nickel porphyrin and hydroporphyrin complexes in the octaethyl, methylated octaethyl, and tetraphenyl series. Reductions were examined in dimethylformamide, methylene chloride, and acetonitrile. The limited solubilities of Ni(OEP) and of the nickel complexes of the tetraphenyl series in some of these solvents precluded several experiments. Potentials are collected in Table I. Some literature data for complexes and measured potentials for the ferricenium/ferrocene couple are included in the table for purposes of comparison.

Table I. Potentials of the Reductions of Free-Base and Ni(II) Porphyrin and Hydroporphyrin Complexes in Selected Solvents

	$E_{1/2}$,[a] V[b]		
complex	CH_3CN	CH_2Cl_2	DMF
H_2(OEP)	−1.44[c,d]		−1.34, −1.79[e]
H_2(OEC)	−1.44, −1.89[f,g]		−1.38
H_2(OEiBC)	−1.70[d]		
H_2(MOEC)	−1.45, −2.05[f]	−1.47[h]	−1.36, −1.84
H_2(DMOEiBC)	−1.77[f,i,j]	−1.80[f,i,k]	−1.62[h]
H_2(TPP)	−1.05[c,l]		−1.08, −1.45[m,n]
H_2(TPC)	−1.12[c,l]		−1.12, −1.52[m,n]
H_2(TPiBC)	−1.52[c,o]		
Ni(OEP)	−1.50[p,q]	−1.46[r]	
Ni(OEC)	−1.46[s]	−1.50[f,i]	−1.39, −2.00
Ni(OEiBC)	−1.54	*[t]	−1.46
Ni(MOEC)	−1.48	−1.55[f,i]	−1.41
Ni(DMOEiBC)	−1.63	*[u]	−1.57
Ni(TPiBC)		−1.55[f,v]	
Fc^+/Fc[w]	0.41	0.45	0.50

[a] $E_{1/2} = 1/2(E_{p,a} + E_{p,c})$. [b] versus SCE at 25 °C in a solution 0.1 M in TBAP with Pt disc working electrode and 100 mV/s scan speed, unless noted otherwise. [c] Butyronitrile solution. [d] Reference 30. [e] Glassy carbon working electrode. [f] $E_{p,c}$ (irreversible). [g] Lit. data:[30] −1.46, −1.9($E_{p,c}$) V. [h] $i_{p,a} < i_{p,c}$. [i] Two-electron process. [j] Lit. data:[34] −1.72 V, one-electron process, in butyronitrile, 200 mV/s scan speed. [k] Two overlapping one-electron processes? [l] Reference 23a. [m] Reference 53b. [n] 0.1 M TEAP. [o] Reference 36. [p] Benzonitrile solution. [q] Reference 23b. [r] Large peak-to-peak separation indicates slow electron transfer. Anodic wave readily lost if electrode not pretreated (see text). [s] Reference 5. [t] Electrocatalytic wave with current equivalent to about 4.9 electrons. Inflection point near −1.5 V. [u] Electrocatalytic wave with current equivalent to about 4.5 electrons. Inflection point near −1.64 V. [v] Cathodic current equivalent to somewhat less than two electrons. [w] Ferricenium/ferrocene couple.

A significant trend was observed in previous examinations of the electrochemistry of free base octaethyl-[30] and tetraphenyl-[23,36] hydroporphyrins. The porphyrin and chlorin of each series were reduced at nearly the same potential (within 30 mV). Reduction of the isobacteriochlorin occurred at a potential roughly 250–420 mV negative of the porphyrin or chlorin. Members of the tetraphenyl series were reduced at potentials 180–360 mV positive of the corresponding macrocycles in the octaethyl series. The data in Table I establish that the trend noted above also applies to the methylated octaethyl hydroporphyrin series. H_2(MOEC) was reduced at essentially the same potential as H_2(OEC). Reduction of the isobacteriochlorin H_2(DMOEiBC) occurred at potentials somewhat negative of H_2(OEiBC).[34,36]

Contrary to the reported behavior in butyronitrile,[34,36] the reduction of H_2(DMOEiBC) in other solvents was not reversible. In acetonitrile and methylene chloride, the reduction current corresponded to a two-electron process. No reoxidation wave was observed upon scan reversal. In some experiments in methylene chloride, the appearance of the voltammogram suggested that the process corresponded to two overlapping one-electron reductions. Alternatively, the wave may correspond to some type of ECE process. The reduction of H_2(DMOEiBC) in DMF was a one-electron process and was better behaved. The reoxidation current was only slightly less than the reduction current. Overall, reduced complexes in the methylated octaethyl hydroporphyrin series appear to be less stable than the corresponding hydrogenated hydroporphyrins. Similarly, the dications of this series are less stable than those of the hydrogenated hydroporphyrins.[37] This contrasts with the resistance of H_2(DMOEiBC) to oxidative dehydrogenation by quinones and with the exceptional stability of the H_2(DMOEiBC) cation radical.[34]

The behavior of nickel porphyrins and hydroporphyrins upon reduction was not typical of other metalloporphyrins. As noted above, nickel porphyrins have only one accessible reduction in these solvents rather than the two typical of other metalloporphyrins.

(36) Richardson, P. F.; Chang, C. K.; Spaulding, L. D.; Fajer, J. *J. Am. Chem. Soc.* **1979**, *101*, 7736.
(37) Stolzenberg, A. M.; Stershic, M. T. *Inorg. Chem.* **1988**, *27*, 1614.

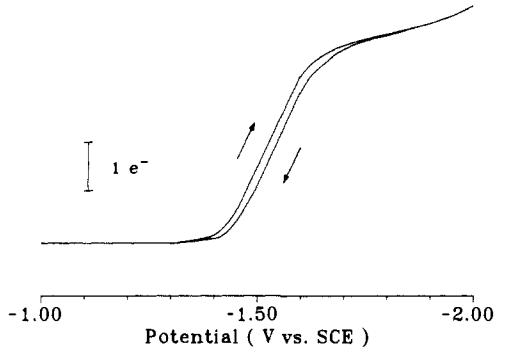

Figure 1. Cyclic voltammogram of Ni(OEiBC) in methylene chloride solution containing 0.1 M TBAP recorded at 100 mV/s. The voltammogram is typical of an electrocatalytic process. The vertical bar, which is included for purposes of comparison, corresponds to the peak height of the one-electron, reversible 1+/0 process measured for the same solution.

This is also true of nickel hydroporphyrins, with the exception of Ni(OEC) in DMF. Another notable difference was that unlike the corresponding free-base complexes, Ni(OEP), Ni(OEC), and Ni(OEiBC) were all reduced at nearly the same potential. The reductions of the nickel complexes displayed greater sensitivity to the previous history of the electrode (and possibly to the presence of trace impurities) than we have observed in our experience with other metalloporphyrins. For some of the nickel complexes, particularly Ni(OEP), failure to pretreat the platinum working electrode with concentrated nitric acid resulted in irreproducible results including loss of the reoxidation wave or a marked increase in the peak-to-peak separation observed in the voltammogram.

The most important difference in the behavior of the nickel complexes upon reduction was the effect of the solvent. All nickel complexes examined underwent a one-electron reversible reduction in nitrile solvents and in DMF. In marked contrast, the nature of the reduction process in methylene chloride solution was strongly dependent upon the identity of the macrocycle. Ni(OEP) was reduced in a one-electron process. Although chemically reversible ($i_{p,c} = i_{p,a}$), the large peak-to-peak separation established that electron transfer was too slow for true Nernstian reversibility. Ni(OEC), Ni(MOEC), and Ni(TPiBC) were irreversibly reduced. The heights of the reduction waves corresponded to approximately two electrons. No reoxidation waves were observed upon scan reversal.

The reductions of Ni(OEiBC) and Ni(DMOEiBC) were dramatically different. The voltammograms for these complexes in methylene chloride, Figure 1, did not have the normal peak-shaped appearance. The *i-E* curve obtained on the scan to negative potentials resembled a polarographic wave (plateau-shaped) and had a limiting current 4.5–5 times that of a reversible one-electron process. An essentially identical *i-E* curve was obtained when the scan direction was reversed. These features are characteristic of a diffusion-controlled electrocatalytic process.[38]

The minimal mechanism that will result in an electrocatalytic process is given in eq 1 and 2. The reduction of OXID, eq 1,

$$\text{OXID} + n\text{e}^- \rightarrow \text{RED}^{n-} \quad (1)$$

$$\text{RED}^{n-} + \text{Z} \xrightarrow{k} \text{OXID} + \text{products} \quad (2)$$

the oxidized form of the catalyst, occurs at the electrode surface. Z is an oxidant which, owing to a substantial overpotential, is not itself reducible at the electrode in the potential range of interest. Z oxidizes RED^{n-} to the oxidized member of the couple, OXID, which can be immediately rereduced at the adjacent electrode. The height (current) and shape of the cyclic voltammetric waveform in such a system depends upon the concentration of the substrate, the sweep rate, and the rate constant for eq 2. High substrate concentrations, large rate constants, and slow sweep rates favor catalytic behavior.

Our observations suggest that the reduced forms of Ni(OEiBC) and Ni(DMOEiBC) react with methylene chloride. Because reactions of methylene chloride are typically slow, this interpretation was confirmed by investigating its effect on the cyclic voltammogram of Ni(OEiBC) in acetonitrile. Addition of several hundred to 1000 equiv of methylene chloride resulted in a change in the voltammogram from that of a reversible one-electron reduction to that observed in neat methylene chloride. Addition of other, more reactive alkyl halides demonstrated that even greater catalytic currents could be obtained at significantly lower substrate concentrations. A figure showing the effect of added CH_3I on the voltammogram of Ni(OEiBC) can be found in ref 27. The total extent of reaction that occurs during a cyclic voltammogram is too small to permit isolation and identification of the product(s) derived from methylene chloride. The product is presumed to be CH_3Cl, however, based upon evidence obtained from bulk reactions of $Ni(OEiBC)^-$ with alkyl halides.[27]

The cyclic voltammograms obtained for reduction of the other nickel complexes in methylene chloride can also be rationalized within the framework of the electrocatalysis scheme. All that is required is that the second-order rate constant for the reaction of the reduced complexes with methylene chloride be "too small" to observe significant catalysis. The critical size of this rate constant is determined in relation to the sweep rate for the experiment. We therefore investigated the effect of the sweep rate on the cyclic voltammograms in methylene chloride. The reduction of Ni(OEiBC) remained catalytic at scan rates as high as 2000 mV/s. In contrast, the reduction of Ni(OEC) only became catalytic at slow scan rates (20 mV/s). Finally, the reduction of Ni(OEP) became chemically irreversible at slow scan rates, but significant enhancement of the reduction current (catalysis) was not observed. It is clear that the rate constant for the reaction of reduced complexes with methylene chloride varies substantially with the macrocycle.

The Generation and Characterization of Reduced Nickel Complexes. Several examples have been reported of the electrocatalytic reduction of alkyl halides by nickel tetraazamacrocyclic complexes. The active catalytic intermediates were nickel(I) complexes.[17,39,40] Given the variation in reactivities observed above, we decided to characterize the species formed upon reduction of the nickel complexes in the three series of ligands.

Bulk electrolyses of the nickel complexes in the octaethyl series (−1.65 V versus SCE, acetonitrile solution) did not afford stable species. Color changes were noted around the working electrode (Pt mesh), but these changes did not persist. It was not clear whether this reflected technical problems with the experiment or the inherent instability of reduced species over the time scale of the electrolysis experiment (30 min to 1 h or more). It should be noted here that bulk electrolysis of F_{430} also failed to produce stable reduced species.[20] The latter were obtained by chemical reduction.

(A) Spectroelectrochemistry. Many species that are inaccessible by bulk electrolysis can be generated and observed in an OTTLE cell.[30] The OTTLE cell design eliminates several problems associated with larger H-cells. Reduction takes place in a thin layer of solution near the electrode. The time scale of the experiment is significantly shorter, because both the quantity of the compound of interest to be electrolyzed and the distance that it need diffuse to the electrode is small. Equally important, the surface tension

(38) (a) Bard, A. J.; Faulkner, L. R. *Electrochemical Methods*; Wiley: New York, 1980; pp 455–461. (b) Nicholson, R. S.; Shain, I. *Anal. Chem.* **1964**, *36*, 706. (c) Saveant, J. M.; Vianello, E. *Electrochim. Acta* **1965**, *10*, 905.

(39) (a) Bakac, A.; Espenson, J. H. *J. Am. Chem. Soc.* **1986**, *108*, 713. (b) Bakac, A.; Espenson, J. H. *J. Am. Chem. Soc.* **1986**, *108*, 719. (c) Bakac, A. Espenson, J. H. *J. Am. Chem.* Soc. **1986**, *108*, 5353. (d) Ram, M. S.; Bakac, A.; Espenson, J. H. *Inorg. Chem.* **1986**, *25*, 3267.

(40) (a) Gosden, C.; Healy, K. P.; Pletcher, D. *J. Chem. Soc., Dalton Trans.* **1978**, 972. (b) Healy, K. P.; Pletcher, D. *J. Organomet. Chem.* **1978**, *161*, 109. (c) Gosden, C.; Pletcher, D. *J. Organomet. Chem.* **1980**, *186*, 401. (d) Gosden, C.; Kerr, J. B.; Pletcher, D.; Rosas, R. *J. Electroanal. Chem.* **1981**, *117*, 101.

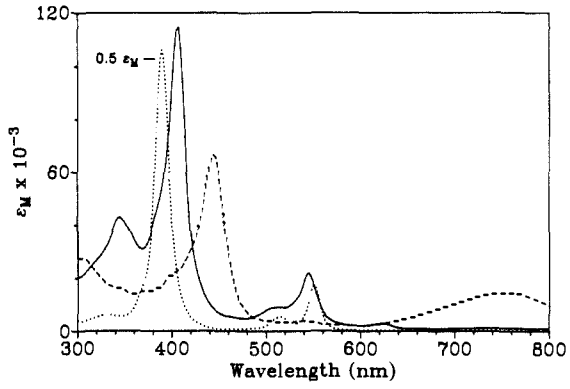

Figure 2. UV–vis spectra of Ni(OEP) (···), Ni(OEP)$^{\bullet-}$ (—), and Ni(OEPH)$^-$ (– – –) in butyronitrile containing 0.1 M TBAP recorded in the OTTLE cell. Ni(OEP)$^{\bullet-}$ was produced by electrolysis at −1.70 V versus SSCE. Ni(OEPH)$^-$ formed after prolonged electrolysis at −2.10 V. For convenience, scale of Ni(OEP) spectrum was reduced by one half. Actual extinctions of Ni(OEP) are twice those shown in figure.

Table II. Quantitative Absorption Spectral Data for Ni(P) Anions[a]

complex	λ_{max}, nm (ϵ, mM)[b]
Ni(OEP)$^{\bullet-}$[c]	344.4 (43.1), 406.2 (114.5), 511.3 (9.2), 544.2 (22.0), 623.2 (2.9)
Ni(OEPH)$^-$[c]	444.6 (66.4), 751.3 (14.8)
Ni^{I}(OEC)$^-$	361.2 (34.1), 382.6 (39.5), 407.1 (35.0), 507.3 (4.2), 589.9 (19.0), 737.6 (3.9)
Ni(OECH)$^-$	358.9 (20.8), 441.5 (5.9), 540.2 (11.9), 704.7 (7.1)
Ni^{I}(OEiBC)$^-$[d]	351.7 (50.7), 374.0 (47.8), 495.7 (9.2), 530.7 (11.0), 571.5 (42.8)

[a] Acetonitrile solution, 0.1 M in TBAP. [b] Relative values of extinction coefficients are known to the precision indicated; absolute values are accurate only to several percent. [c] Butyronitrile solution, 0.1 M in TBAP. The presence of TBAP did not seem to affect the spectra. Similar spectra were obtained by amalgam reduction of electrolyte free solutions. [d] ϵ_M values may be somewhat low owing to slight precipitation of complex.

of the thin layer prevents mixing by convection. It is only necessary to "preelectrolyze" the oxidizing species present in the region immediately around the working electrode (about 100 μL). Diffusional mixing of the reduced complex with oxidizing species, whether present as impurities in the bulk solvent or generated at the counter electrode, is slow on the time scale of the experiment.

1. Ni(OEP). Electrolysis of Ni(OEP) in butyronitrile at −1.70 V led to changes in the UV–vis spectrum, Figure 2. The Soret and visible bands of Ni(OEP) at 391 and at 515 and 551 nm, respectively, were replaced by new bands of lesser intensity at 344, 406, 511, 544, and 623 nm. The extinction coefficients of the major bands of Ni(OEP)$^-$, and other reduced nickel complexes, are collected in Table II. The changes in the spectrum upon reduction of Ni(OEP), particularly the red shift of the Soret band, are analogous to those observed upon reduction of Zn(TPP).[41,42] This is consistent with formation of a metalloporphyrin anion radical,[43] an assignment confirmed in experiments described below. Oxidation of Ni(OEP)$^{\bullet-}$ at 0.0 V (after 5–10 min at −1.70 V) led to quantitative recovery of Ni(OEP). Repeated reduction–oxidation cycles did not lead to degradation of the spectra, demonstrating the reversibility of the first reduction under these conditions.

Reduction of Ni(OEP) at −2.10 V, the extreme limit of potential accessible in our system, resulted initially in rapid formation of Ni(OEP)$^{\bullet-}$. At longer times, the anion radical disappeared, and a second product complex was formed. The current required to form this complex could not be determined, due to the high background current at −2.10 V. The spectrum of the complex, Figure 2, consisted of a band of medium intensity at 445 nm and a rather broad, weak band at 752 nm. These features are characteristic of the spectra of phlorin complexes, suggesting that the second complex is the phlorin anion, Ni(OEPH)$^-$, whose structure is shown below. The ^{1}H NMR spectrum of the complex, discussed later, proved this assignment.

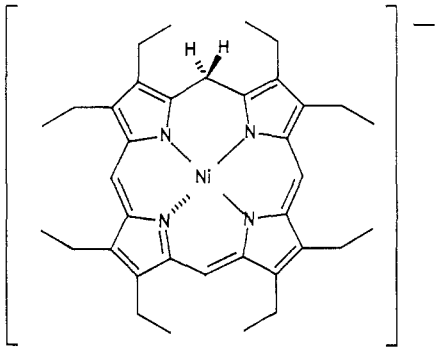

Ni(OEPH)$^-$

Ni(OEPH)$^-$ was not reoxidized when the applied potential was increased to −1.55 V, a potential negative of the reduction of Ni(OEP) to the anion radical. The potential was slowly increased. The oxidation current became detectable when the potential was significantly positive of the potential of the Ni(OEP)/Ni(OEP)$^{\bullet-}$ couple. Oxidation became rapid at potentials greater than −1.00 V. Ni(OEPH)$^-$ was converted directly to Ni(OEP) without intermediate formation of Ni(OEP)$^{\bullet-}$. Several cycles between Ni(OEP) and Ni(OEPH)$^-$ were performed without detectable loss of complex.

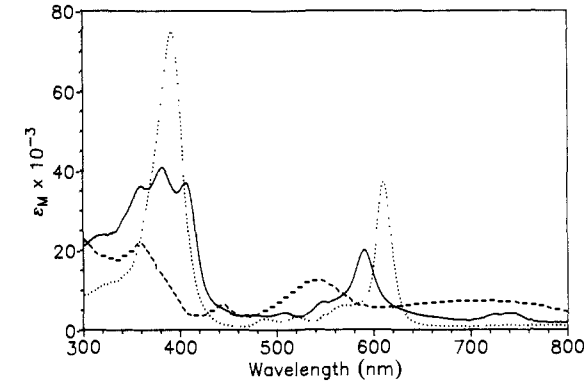

Figure 3. UV–vis spectra of Ni(OEC) (···), Ni^{I}(OEC)$^-$ (—), and Ni(OECH)$^-$ (– – –) in acetonitrile containing 0.1 M TBAP recorded in the OTTLE cell. Ni^{I}(OEC)$^-$ was produced by electrolysis at −1.55 V. Ni(OECH)$^-$ formed after prolonged electrolysis at −2.10 V.

2. Ni(OEC). Electrolysis of Ni(OEC) in acetonitrile at −1.55 V afforded Ni(OEC)$^-$, whose UV–vis spectrum is shown in Figure 3. The principle visible band of Ni(OEC)$^-$ was at 590 nm, 24 nm to the blue of the visible band in Ni(OEC). The Soret band also blue shifted and split into three overlapping bands of near equal intensity at 361, 382, and 407 nm. Finally, a weak, broad band was observed at 737 nm. Oxidation of Ni(OEC)$^-$ at 0.00 V (after 5–10 min at −1.55 V) led to quantitative recovery of Ni(OEC). The complex was stable to repeated reduction–oxidation cycles.

The UV–vis spectrum does not provide a clear indication of the electron distribution in Ni(OEC)$^-$. The blue shifts of the Soret and visible bands suggest that the reduction is metal centered, but the long wavelength band at 737 nm and drop in extinction coefficients of the absorption bands are more indicative of a macrocycle-centered reduction. Comparisons of the spectrum with those of two reported metallochlorin anion radicals were ambiguous. The spectrum is quite unlike that of Ni(TMC)$^{\bullet-}$,[24] whose bands broadened and bleached appreciably, but does bear some resemblance to the spectrum of the anion radical of chlorophyll a.[44] For further comparison, we reduced two metallochlorins with

(41) Closs, G. L.; Closs, L. E. *J. Am. Chem. Soc.* **1963**, *85*, 818.
(42) Lanese, J. G.; Wilson, G. S. *J. Electrochem. Soc.* **1972**, *119*, 1039.
(43) Reed, C. A. *Adv. Chem. Ser.* **1982**, 333.

redox inactive metals, Mg(OEC) and Zn(OEC), to their respective anion radicals in the OTTLE cell. The spectra obtained resembled that of Ni(TMC)$^{\bullet-}$ more closely than that of Ni(OEC)$^-$. Bands red shifted a few nm and dropped considerably in intensity (by about a factor of 5). A small band also appeared at 750 nm in the spectrum of Zn(OEC)$^{\bullet-}$. Overall, the most appropriate spectral comparison for Ni(OEC)$^-$ may be with Fe(TPP)$^-$. The best description of Fe(TPP)$^-$ is a resonance hybrid of an iron(I) porphyrin with some contribution from an iron(II) porphyrin anion radical.[43] EPR,[45,46a] resonance Raman,[46] NMR,[47] and Mössbauer[43] data support the iron(I) description of this complex, but UV–vis[43] and crystallographic[48] data suggest a significant donation of electron density to the macrocycle. In analogy with this situation, the EPR spectrum of Ni(OEC)$^-$, which is discussed below, supports a nickel(I) formulation for Ni(OEC)$^-$.

The behavior of Ni(OEC) when electrolyzed at −2.10 V in acetonitrile was similar to that of Ni(OEP) at the same potential. A second product complex was slowly formed after the initial rapid formation of Ni^{I}(OEC)$^-$. The UV–vis spectrum of the second complex was analogous to that of Ni(OEPH)$^-$, the second Ni(OEP) reduction product. Broad, weak absorption bands were observed at 359, 540, and 704 nm. Identification of the product as the chlorin–phlorin (pyrroline ring and saturated meso position) complex Ni(OECH)$^-$ is verified by its ^{1}H NMR spectrum, discussed below. As expected, Ni(OECH)$^-$ was not oxidized when the applied potential was increased to −1.55 V. At potentials greater than −1.00 V, the complex was oxidized directly to Ni(OEC). Several cycles between Ni(OEC) and Ni(OECH)$^-$ were performed without degradation of the complex.

3. Ni(OEiBC). Reduction of Ni(OEiBC) in acetonitrile at −1.70 V resulted in two significant changes in the UV–vis spectrum. (The UV–vis spectrum obtained has been published in ref 28.) All bands shifted approximately 20 nm to the blue. The visible bands at 520, 548, and 593 nm in Ni(OEiBC) were replaced by bands at 496, 531, and 571 nm in the spectrum of Ni(OEiBC)$^-$. The Soret band at 385 nm also shifted upon reduction and split into several overlapping bands with distinct maxima at 352 and 374 nm and a shoulder at 320 nm. The extinction coefficients and widths of the bands in the spectra of Ni(OEiBC) and Ni(OEiBC)$^-$ were comparable. The spectrum of the latter suggests that it is the nickel(I) complex Ni^{I}(OEiBC)$^-$, an assignment confirmed below. No degradation of the complex was observed after repeated reduction–oxidation cycles. Ni^{I}(OEiBC)$^-$ did not undergo further reduction at more negative potentials, unlike Ni(OEP) and Ni(OEC).

(B) Chemical Reductions. We investigated several classes of reducing agents. Dilute sodium amalgam was found to be the reductant of choice in most situations. It has two significant advantages over the radical anions of aromatic hydrocarbons: it does not absorb at wavelengths that are of interest, and reduced complexes can be separated from excess amalgam and its by-products by decanting. It was not possible to use stoichiometric amounts of amalgam on the small reaction scale employed here (10^{-6}–10^{-5} mol or less). The potential of sodium amalgam (approximately −2.05 V versus SCE in acetonitrile and THF[49]) is considerably negative of the potentials of the nickel complexes of interest. Thus, multiple electron reductions were possible in the presence of excess amalgam.

1. Ni(OEP). Reduction of an acetonitrile or THF solution of Ni(OEP) by excess sodium amalgam resulted in color changes from red to orange and finally to yellow-brown. UV–vis spectra recorded during the reaction showed that the reduction did not proceed in discrete steps. Small but definite deviations from isosbestic behavior established that at least three species were present. The largest deviations occurred in two regions centered near 350 and 420 nm. Both are close to the wavelengths of peaks associated with Ni(OEP)$^{\bullet-}$. This suggests that a small steady-state concentration of the anion radical Ni(OEP)$^{\bullet-}$ was present during the reduction. The final UV–vis spectrum was identical with that obtained by reduction of Ni(OEP) at −2.10 V in the OTTLE cell. On the basis of this spectrum, we suggested above that the phlorin anion complex Ni(OEPH)$^-$ had been formed.

Phlorins have been prepared by chemical,[41,50,51] electrochemical,[42,52,53] photochemical,[54,55] and pulse radiolytic[56] reduction of porphyrins. These diamagnetic complexes result from meso protonation of porphyrin dianions,[41] which occurs readily even in apparently aprotic solvents.[42,57] Phlorins have not yet been characterized by X-ray diffraction methods. Hence, the site of protonation has been deduced from spectroscopic data.[41,50,51,55] An important consequence of the saturation of a meso position is that the macrocycle ring current is interrupted. Meso protons are found substantially upfield of their position in the porphyrin.[41,50a,51,52b,55] Other peaks shift upfield by notable, but lesser, amounts. Phlorins are stable complexes[50b] but are rapidly reoxidized to porphyrins by oxygen, iodine, quinones, and other similar oxidants.[50,51,54] Protonation of the porphyrin dianion affords sufficient stabilization, though, that the reduction potential of the porphyrin/phlorin anion couple is positive of the potential of the porphyrin/porphyrin anion radical couple.[42,53] As a consequence, porphyrin and phlorin do not comproportionate to yield porphyrin anion radicals. Rather, phlorins are formed by the disproportionation of anion radicals in the presence of a proton source.[41,53a] The comproportionation reaction was reported to be driven partially to completion by photochemical means, however.[58]

The properties and reactivity of Ni(OEPH)$^-$, the final product of the amalgam reduction, were entirely consistent with those described above for phlorin complexes. Solutions of Ni(OEPH)$^-$ were EPR silent, both at 77 K and at room temperature. Three singlets in the ^{1}H NMR spectrum at 7.22, 6.70, and 3.03 ppm that occur in a 2:1:2 ratio provide strong evidence for the phlorin structure, which has 2-fold rather than 4-fold symmetry. These peaks are assigned to the 10,20-H, 15-H, and two 5-H meso protons, respectively, and have shifted some 3–7 ppm upfield of their positions in Ni(OEP). All other peaks in the spectrum were shifted upfield of their positions in Ni(OEP) by lesser amounts. Solutions of Ni(OEPH)$^-$ were indefinitely stable (months) when sealed in vacuo but were immediately reoxidized to Ni(OEP) upon exposure to air. Solutions of Ni(OEP) and Ni(OEPH)$^-$ did not comproportionate to Ni(OEP)$^-$ when mixed. The UV–vis spectrum of the resulting solution was simply the superposition of the spectra of the two individual solutions. The resulting solution was also EPR silent. This was consistent with the observation, discussed above, that reoxidation of the second reduction product in the OTTLE occurred only at potentials positive of the Ni(OEP)/Ni(OEP)$^-$ couple.

(44) Fujita, I.; Davis, M. S.; Fajer, J. *J. Am. Chem. Soc.* **1978**, *100*, 6280.
(45) (a) Cohen, I. A.; Ostfeld, D.; Lichenstein, B. *J. Am. Chem. Soc.* **1972**, *94*, 4522. (b) Lexa, D.; Momenteau, M.; Mispelter, J. *Biochim. Biophys. Acta* **1974**, *338*, 151. (c) Kadish, K. M.; Larson, G.; Lexa, D.; Momenteau, M. *J. Am. Chem. Soc.* **1975**, *97*, 282.
(46) (a) Srivatsa, G. S.; Sawyer, D. T.; Boldt, N. J.; Bocian, D. F. *Inorg. Chem.* **1985**, *24*, 2123. (b) Teraoka, J.; Hashimoto, S.; Sugimoto, H.; Mori, M.; Kitagawa, T. *J. Am. Chem. Soc.* **1987**, *109*, 180.
(47) Hickman, D. L.; Shirazi, A.; Goff, H. M. *Inorg. Chem.* **1985**, *24*, 563.
(48) Mashiko, T.; Reed, C. A.; Haller, K. J.; Scheidt, W. R. *Inorg. Chem.* **1984**, *23*, 3192.
(49) Horner, L.; Schmitt, R.-E. *Z. Naturforsch., B: Anorg. Chem., Org. Chem.* **1982**, *37B*, 1163.
(50) (a) Woodward, R. B. *Ind. Chim. Belg.* **1962**, *11*, 1293. (b) Woodward, R. B. *Pure Appl. Chem.* **1961**, *2*, 395. (c) Woodward, R. B.; Ayer, W. A.; Beaton, J. M.; Bickelhaupt, F.; Bonnett, R.; Buchschacher, P.; Closs, G. L.; Dutler, H.; Hannah, J.; Hauck, F. P.; Ito, S.; Langermann, A.; Le Goff, E.; Leimgruber, W.; Lwowski, W.; Sauer, J.; Valenta, Z.; Volz, H. *J. Am. Chem. Soc.* **1960**, *82*, 3800.
(51) Sugimoto, H. *J. Chem. Soc., Dalton Trans.* **1982**, 1169.
(52) (a) Inhoffen, H. H.; Jäger, P. *Tetrahedron Lett.* **1964**, 1317. (b) Inhoffen, H. H.; Jäger, P.; Mählhop, R.; Mengler, C.-D. *J. Liebigs Ann. Chem.* **1967**, *704*, 188.
(53) (a) Peychal-Heiling, G.; Wilson, G. S. *Anal. Chem.* **1971**, *43*, 545. (b) Peychal-Heiling, G.; Wilson, G. S. *Anal. Chem.* **1971**, *43*, 550.
(54) (a) Mauzerall, D. *J. Am. Chem. Soc.* **1960**, *82*, 1832. (b) Mauzerall, D. *J. Am. Chem. Soc.* **1962**, *84*, 2437.
(55) Suboch, V. P.; Shul'ga, A. M.; Gurinovich, G. P.; Glazkov, Yu. V.; Zhuravlev, A. G.; Sevchenko, A. N. *Doklady Phys. Chem.* **1972**, *204*, 419.
(56) Harel, Y.; Meyerstein, D. *J. Am. Chem. Soc.* **1974**, *96*, 2720.
(57) Hush, N. S.; Rowlands, J. R. *J. Am. Chem. Soc.* **1967**, *89*, 2976.
(58) Mauzerall, D.; Feher, G. *Biochim. Biophys. Acta* **1964**, *88*, 658.

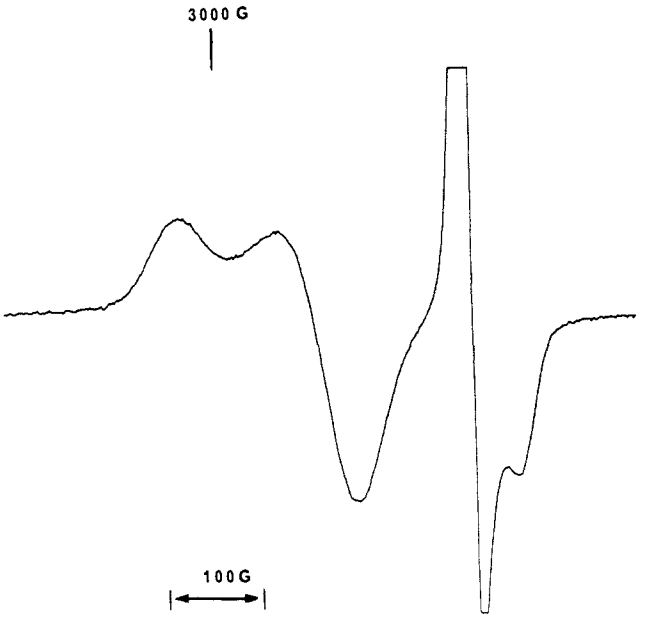

Figure 4. EPR spectrum of a mixture of $Ni^{I}(OEC)^-$ and excess sodium tetracenide in THF glass at 100 K. The tetracenide peak is off-scale.

We attempted to find reductants and/or reaction conditions that would lead to production of significant concentrations of $Ni(OEP)^{\bullet-}$. In all systems investigated, the UV–vis spectra suggested that reduction proceeded directly to $Ni(OEPH)^-$. Apparently, disproportionation or further reduction of $Ni(OEP)^{\bullet-}$ is faster than the initial reduction of Ni(OEP). However, a radical EPR signal with $g = 2.003$ ($\Delta H_{p-p} = 23$ G) was detected in incompletely reduced solutions. Resolved hyperfine splittings were not observed. A weak EPR signal with the same g value and line width was generated by the photochemically driven comproportionation reaction of Ni(OEP) and $Ni(OEPH)^-$.[58] In this experiment, a butyronitrile solution of the two complexes in a quartz EPR tube was irradiated for about 10 min with long wavelength UV light in a Rayonet reactor and then was immediately frozen in liquid nitrogen. Both EPR experiments confirm that $Ni(OEP)^-$ is an anion radical.[59]

2. Ni(OEC). The color of solutions of Ni(OEC) in acetonitrile or THF changed from blue-green to an intense royal blue upon reduction by sodium amalgam. As in the amalgam reduction of Ni(OEP), UV–vis spectra revealed small but definite deviations from isosbestic behavior. Deviations were most notable near 590 nm, the wavelength of the visible band of $Ni(OEC)^-$. The extent of the deviation depended upon reaction conditions. Deviations were minor in experiments conducted in THF solution. In acetonitrile solution, a small but discernable peak initially grew in at 590 nm but disappeared in the later stages of the reaction. The final UV–vis spectrum was identical with that obtained upon reduction of Ni(OEC) at −2.10 V in the OTTLE cell, a spectrum which we have attributed to the chlorin–phlorin complex, $Ni(OECH)^-$.

The properties and reactivity of $Ni(OECH)^-$ were consistent with those expected for a phlorin-like complex and were analogous to those of $Ni(OEPH)^-$. $Ni(OECH)^-$ was readily oxidized by air but did not comproportionate with Ni(OEC). In agreement with the expected loss of 2-fold symmetry upon reduction of Ni(OEC) to $Ni(OECH)^-$, three singlets (1 H each) were observed in the ^{1}H NMR spectrum at 6.94, 5.92, and 5.87 ppm and were assigned to the meso protons of $Ni(OECH)^-$. These are shifted 2.2 ppm upfield of their respective positions in Ni(OEC)[5] and have chemical shifts similar to those reported for the meso protons of other chlorin–phlorins.[52b,55] Further evidence for the interrupted ring current and reduction in symmetry of $Ni(OECH)^-$ were found in the upfield shifts of all other peaks, the inequivalence of the β-H protons, and the inequivalence of the two pyrroline ring methyl groups.

Two isomeric chlorin–phlorin complexes can be produced from OEC by saturation of either the meso positions adjacent to (C-5,20) or remote from (C-10,15) the pyrroline ring. Each isomer has three inequivalent meso protons. Only three meso singlets were detected in the spectrum of $Ni(OECH)^-$. Thus, the reaction was selective for one product, possibly the thermodynamically preferred one.[50a] Assuming that the sense of the shift difference between the OEC 5,20- and 10,15-meso protons does not change upon conversion to OECH, observation of two meso protons upfield and only one downfield established that OECH was saturated at C-10. This structure is illustrated in the drawing below. The

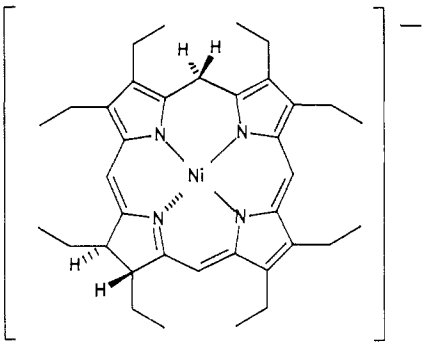

$Ni(OECH)^-$

same selectivity was reported for the products of the electrochemical reduction of several C-5 substituted chlorins.[52b] Different selectivities were observed, though, in the photochemical reduction of one of these chlorins[55] and the electrochemical reduction of C-5 unsubstituted chlorins.[52b]

Several different reducing agents with potentials positive of sodium amalgam were examined to find conditions that afforded $Ni(OEC)^-$. Magnesium and aluminum amalgams gave somewhat increased absorptions at 590 nm but led to precipitation of the product. Reduction with sodium anthracenide proceeded directly to OECH. Eventually, we found that in THF solution reaction of Ni(OEC) with excesses of the anion radicals of rubrene and tetracene afforded substantial concentrations of $Ni(OEC)^-$ without production of $Ni(OECH)^-$. The UV–vis spectra of the resulting solutions clearly showed absorption bands corresponding to $Ni(OEC)^-$ superimposed upon the bands of Ni(OEC), the anion radical, and its neutral aromatic. The potentials of rubrene and tetracene ($E_{1/2} = -1.41$ and -1.58 V versus SCE in DMF,[60] respectively) are probably close to the potential of Ni(OEC) in THF. Of the two, tetracene was a sufficiently strong reducing agent to permit near total conversion of Ni(OEC) to $Ni(OEC)^-$ with a reasonable excess of the anion radical. Reaction of Ni(OEC) with anion radicals of hydrocarbons with lower potentials (fluoranthene, $E_{1/2} = -1.76$ V versus SCE in DMF[60]) led to significant quantities of $Ni(OECH)^-$.

The EPR spectrum of $Ni(OEC)^-$ obtained by reduction of Ni(OEC) with excess tetracene anion radical is shown in Figure 4. In addition to the spectrum of tetracene anion radical (truncated peak at $g = 2.00$) a rhombic spectrum with g values of 2.19, 2.10, and 1.98 is clearly present. These g values require the presence of a metal-centered spin, which provides strong evidence that $Ni(OEC)^-$ is $Ni^{I}(OEC)^-$. The EPR spectra of nickel(I) tetraazamacrocyclic complexes generally are axial, but

(59) It has been suggested[57] that the product of irradiation of the porphyrin–phlorin mixture is the neutral phlorin radical rather than the porphyrin anion radical. Optical absorption difference spectra recorded during the irradiation appear to be consistent with production of the anion radical, however.[58] Furthermore, unless the porphyrin anion radical and the phlorin radical coincidentally have rather similar line widths and g values, our results demonstrate that the suggestion in the literature is incorrect. The potential required for formation of the neutral phlorin radical can be estimated[42] to lie in a range such that the phlorin radical could not be present in the incompletely reduced Ni(OEP) solution.

(60) Mann, C. K.; Barnes, K. K. *Electrochemical Reactions in Nonaqueous Systems*; Marcel Dekker: New York, 1980; pp 31–103.

the spectra of some five-coordinate Ni(I) complexes are rhombic.[16] Interactions of $Ni^{I}(OEC)^{-}$ with tetracene or the delocalization of electron density onto the macrocycle that is suggested by the UV–vis spectrum (see above) may be responsible for the rhombicity of $Ni^{I}(OEC)^{-}$.

3. Ni(OEiBC). Sodium amalgam reductions of Ni(OEiBC) in acetonitrile or THF solution were accompanied by a color change from blue-purple to violet. The UV–vis spectra of the final product was identical with that of $Ni(OEiBC)^{-}$ generated by electrolysis in an OTTLE cell. Isobestic points were maintained throughout the reduction. In the presence of excess amalgam, $Ni(OEiBC)^{-}$ was indefinitely stable (>24 h) to further reduction or to disproportionation to phlorin-like complexes.

The EPR spectrum of $Ni(OEiBC)^{-}$ in 2-MeTHF glass[28] unequivocally confirmed the $Ni^{I}(OEiBC)^{-}$ formulation proposed above. The anisotropy and hyperfine coupling of both transitions to the four $S = 1$ nitrogens of OEiBC are consistent with an unpaired electron in the $d_{x^2-y^2}$ orbital of a square-planar nickel(I) complex.[14] The observed g values of 2.201 and 2.073 and the hyperfine coupling of 9.8 G are similar to those of reduced F_{430} species, both in vivo[13] and in vitro,[20] and Ni(I) macrocyclic complexes.[14,16,17] The anisotropy of $Ni^{I}(OEiBC)^{-}$ is less pronounced than that of the other complexes, however.

4. Ni(DMOEiBC). The changes in the UV–vis spectra during the sodium amalgam reduction of Ni(DMOEiBC) in THF were similar to those observed during reduction of Ni(OEC). Isosbestic points were not maintained. The absorbance in a region to the blue of the visible band increased. Eventually, a distinct shoulder was observed at 572 nm, a wavelength close to that of the main visible band of $Ni^{I}(OEiBC)^{-}$ (571 nm). Later, the absorbance near 572 nm decreased, and the shoulder disappeared. The final spectrum was reminiscent of a chlorin–phlorin spectrum. It consisted of a medium intensity band (λ_{max} < 300 nm, 318 nm sh) and a broad, weak band (455 nm, 510 nm sh) that tailed to wavelengths in excess of 800 nm. The final product was EPR silent.

The results suggest that Ni(DMOEiBC) is first reduced to $Ni^{I}(DMOEiBC)^{-}$. This conclusion is supported by the efficiency of the electrocatalytic reduction of methylene chloride catalyzed by Ni(DMOEiBC), which is comparable to that catalyzed by Ni(OEiBC). $Ni^{I}(DMOEiBC)^{-}$ apparently disproportionates rapidly or is further reduced under the reaction conditions to afford an isobacteriochlorin–phlorin or a similar hexahydroporphyrin. We were unable to obtain additional confirmation of these conclusions because the experiments described above exhausted our limited supplies of Ni(DMOEiBC) and its oxoporphyrin precursor 3,3,8,8,12,13,17,18-octaethyl-2,7-porphindione.

5. Ni(TPP) Series. Sodium amalgam reductions of Ni(TPP), Ni(TPC), and Ni(TPiBC) were exceedingly complicated. The reductions proceeded neither in clean stages from one reduced complex to another nor to a single final product. Regardless of the complexity, none of the data suggest that a nickel(I) intermediate was involved in these reactions.

Studies of the electrochemical reduction of Zn(TPP) in DMF have shown that the phlorin anion $Zn(TPPH)^{-}$ can be reduced to the paramagnetic phlorin dianion $Zn(TPPH)^{2-}$ at a potential of approximately −1.9 V.[42] This is about the same potential as required for reduction of $Zn(TPP)^{\bullet-}$ to $Zn(TPP)^{2-}$. In addition, the phlorin dianion undergoes slow, proton-transfer-dependent reduction at this potential. Because the potentials for reduction of Zn(TPP) and Ni(TPP) are similar,[25] the reductions of the anion radical[24] $Ni(TPP)^{\bullet-}$ to $Ni(TPP)^{2-}$, of $Ni(TPPH)^{-}$ to $Ni(TPPH)^{2-}$, and of protonated $Ni(TPPH)^{2-}$ are all expected to occur at approximately −1.9 V. This is positive of the potential of sodium amalgam.[49] Thus, a multitude of species could be present during the reductions of the nickel tetraphenylporphyrin and -hydroporphyrin complexes.

UV–vis spectra obtained during the reductions of Ni(TPP), Ni(TPC), or Ni(TPiBC) were consistent with the presence of several species during the reduction. In no case were isosbestic points observed. Changes in the spectra of the Ni(TPC) reduction were most distinct and were consistent with the initial production of $Ni(TPC)^{\bullet-}$. The absorbance increased at 455, 552, 628, and 740 nm, wavelengths appropriate for the red-shifted Soret and visible bands of metalloporphyrin anion radicals.[24,41,42] With time, the absorbance in these regions decreased and increased in regions characteristic of the chlorin–phlorin spectrum.

The final UV–vis spectra (little change over a 30 min or so time period) of the reductions were not very informative. The final spectrum for the reduction of Ni(TPP) had new features at 444, 525, and 767 nm. The relative extinctions of these bands could not be judged owing to the presence of other species. The positions of these bands bear a closer resemblance to those of $Zn(TPPH)^{2-}$ than to those of $Zn(TPPH)^{-}$,[42] suggesting that $Ni(TPPH)^{2-}$ rather than $Ni(TPPH)^{-}$ is the major species present in the final product. The final spectra of Ni(TPC) and Ni(TPiBC) were both very broad, nearly featureless, and weak. Maxima were observed at 317, 370 (sh), 553, and 682 nm for reduced Ni(TPC) and at 311, 353 (sh), 505, and 633 nm for reduced Ni(TPiBC).

The anion radical and phlorin dianion, two of the species that may be present, are paramagnetic and have observable EPR spectra. A very limited number of examples suggest that the spectra of these radicals are different.[42] Porphyrin anion radicals appear to have line widths of about 20 G and lack hyperfine structure.[25] The phlorin dianion, on the other hand, has a considerably narrower signal (6 G) with hyperfine structure.[42,57]

The EPR spectrum (room temperature) of the solution obtained at the end of the reduction of Ni(TPP) was symmetric about g = 2.005, had a peak-to-peak width of 16 G, and exhibited a nine line hyperfine pattern (2.8 G coupling constant) consistent with coupling to the eight equivalent, $S = 1/2$ β-protons. Our g value agrees within error with the value reported for electrochemically generated $Ni(TPP)^{\bullet-}$.[24] No line width or hyperfine structure was reported for the EPR spectrum of authentic $Ni(TPP)^{\bullet-}$. While our observed line width is about that expected for $Ni(TPP)^{\bullet-}$,[25] the presence of hyperfine structure is more suggestive of $Ni(TPPH)^{2-}$.[42]

The EPR spectra of solutions of reduced Ni(TPC) and Ni(TPiBC) both had g = 2.006. Both lacked hyperfine structure, were decidedly nonsymmetric, and had a shoulder on the low field side of the transition. Peak-to-peak line widths were 13 and 10 G, respectively. The shoulders could have resulted from overlap of a narrower phlorin dianion and broader anion radical spectra, if both species were present in solution. On the other hand, the decrease in line width with saturation of the macrocycle was consistent with that observed on going from Zn(TPP) to Zn(TPC).[25]

Overall, our data suggest that each complex is initially reduced to a nickel(II) anion radical and subsequently to phlorin anion and dianion species. Full characterization of the species formed in these reductions would require a thorough spectroelectrochemical investigation (UV–vis and EPR). This is beyond the scope of the present investigation.

Discussion

The nickel tetrapyrrole complexes investigated here can be divided into three classes based upon the mechanism of their reduction. The first class consists of complexes initially reduced to nickel(II) anion radicals. Disproportionation and/or further reduction lead to formation of phlorins. (Disproportionation is slow on the time scale of cyclic voltammetry.) Ni(OEP) and the entire tetraphenyl series exemplify this behavior. The second class is reduced to nickel(I) complexes that are thermodynamically unstable relative to phlorin complexes. The latter are subsequent products. Ni(OEC) and Ni(DMOEiBC) exhibit this reactivity. The sole member of the third class, Ni(OEiBC), is reduced to a thermodynamically stable nickel(I) complex. Given the ease and rapidity with which the other nickel(I) complexes form phlorins, it would seem unreasonable to attribute the persistence of $Ni^{I}(OEiBC)^{-}$ to the kinetic inacessibility of the corresponding phlorin complex.

The three reactivity classes are *not* defined by the saturation level of the macrocycle. The isobacteriochlorin complexes Ni(TPiBC), Ni(OEiBC), and Ni(DMOEiBC) each belong to a

different class. Apparently, the substituents on the macrocycle play an important role in defining the reactivity of the complex. The source of some of these effects will be considered in the discussion below.

Factors Determining the Site of the Initial Reduction. To a first approximation, the site of reduction is determined by electronic energies and the character of the LUMO orbital. The candidates for the LUMO of the nickel tetrapyrrole complexes are the MOs derived principally from the nickel $d_{x^2-y^2}$ orbital (transforms as B_{1g}[61]) and from the tetrapyrrole E_g[61] π^* orbital. It is obvious that reduction will lead to a nickel(I) complex if the $d_{x^2-y^2}$ orbital lies lower in energy than the π^* orbital and to an anion radical if the order is reversed. The relative energies of these two orthogonal orbitals are not obvious, however. Moreover, it is the order of orbital energies in the reduced complexes that is more important. This could differ from the order in the neutral complex in ways that are difficult to anticipate. The energies of both orbitals are variable and are controlled by different sets of influences. We discuss the influences on each orbital separately.

1. Macrocycle Reduction Potential. In tetrapyrrole complexes of redox innocent metals, the potential at which the complex is reduced reflects the energy of the π^* orbital of the complex. The potential of the complex depends primarily on the potential of the free-base macrocycle and to a lesser extent on the electrostatic effect of the coordinated metal.[22,23,30]

Reduction potentials of free-base tetrapyrrole macrocycles are markedly dependent on their saturation level. Isobacteriochlorins are reduced at potentials significantly negative of porphyrins and chlorins. The −1.70 V reduction potential of H_2(OEiBC)[30] (versus −1.45 V for H_2(OEP) and H_2(OEC)[30]) helps insure that the E_g π^* orbitals of OEiBC lie higher in energy than the nickel $d_{x^2-y^2}$ orbital and, therefore, that nickel is the site of reduction.

Reduction potentials of tetrapyrrole macrocycles are also affected by the identity of the peripheral substituents.[22,23] The presence of electron-withdrawing phenyl substituents and the absence of electron-releasing β-alkyl groups in H_2(TPP), H_2(TPC), and H_2(TPiBC) lead to reduction of these complexes at potentials[36,53b] that are significantly anodic of the respective octaethyl complexes.[30] It is not surprising that all of the nickel complexes in the tetraphenyl series underwent macrocycle-centered reductions.

The energy of the π^* orbitals in nickel(I) complexes is affected by an additional interaction. The empty OEiBC π^* and filled nickel d_{xz} and d_{yz} orbitals have the proper symmetry and relative energies to permit them to mix. Mixing of the π^* orbital with the predominantly nickel d_π MO stabilizes this filled orbital and has the effect of delocalizing electron density from nickel(I) into the tetrapyrrole π^*. Concurrently, the interaction destabilizes the predominantly π^* MO, which rises even higher in energy relative to the $d_{x^2-y^2}$ orbital. The 20-nm blue shift of the main visible band ($\pi \rightarrow \pi^*$ transition) in the UV–vis spectrum of Ni^I(OEiBC)$^-$ relative to Ni(OEiBC) is consistent with the destabilization of the π^* orbital anticipated upon mixing.

2. Ligand Field. The energies of the π^* orbitals of Ni(OEP) and Ni(OEC) should be similar because H_2(OEP) and H_2(OEC) are reduced at the same potential.[30] Yet, Ni(OEP) undergoes a macrocycle-centered reduction, and Ni(OEC) is reduced at nickel. The $d_{x^2-y^2}$ orbital of Ni(OEC) must lie lower in energy than the π^* orbitals of either complex for this to occur. In turn, the π^* orbitals are lower in energy than the $d_{x^2-y^2}$ orbital of Ni(OEP). Because the nickel $d_{x^2-y^2}$ orbital is metal–ligand σ antibonding in the square-planar coordination geometry of these complexes, the inescapable conclusion is that *hydroporphyrins and porphyrins produce different ligand fields* for a coordinated nickel ion.

The observation that hydroporphyrins and porphyrins differ as ligands is new and unanticipated. In previous investigations, hydroporphyrins and porphyrins were notable for providing remarkably similar ligand fields. A case in point is the chemistry of the iron complexes, the metal complexes which have been investigated most thoroughly. Although iron hydroporphyrin complexes have somewhat different anisotropies than the corresponding porphyrin complexes,[7,62,63] the spin states of these complexes and spin state equilibria that they undergo upon changes in ligation were unaffected by the macrocycle.[62] Similarly, iron-centered properties including Fe(III)/Fe(II) potentials,[62,64–66] axial ligand stretching frequencies in ferrous macrocycle CO[62] and NO[66] complexes, and CO affinities[67] were not significantly macrocycle dependent.

One important property differentiates iron and nickel: the size of these ions in relation to the macrocycle hole. The center-to-nitrogen distance is 2.01 Å in the hypothetical porphyrin of minimal strain.[68] A hole of this size readily accommodates in-plane coordination of low-spin ferric and ferrous iron. High-spin ferric ion is invariably displaced far enough out of plane (toward the coordinated anion) that rather little expansion of the porphyrin core is required. In contrast, the optimal Ni–N distances for nickel(II) with unidentate ligands is 1.88 Å in low-spin complexes and 2.11 Å in high-spin complexes.[9] Thus, low-spin nickel(II) is "too small" for the porphyrin of minimal strain, while the high-spin ion is "too large". It is this mismatch of sizes that allows the difference in ligand fields of porphyrins and hydroporphyrins to become apparent.

The radius of a nickel(I) ion will be as large or larger than that of a high-spin nickel(II) ion. Both have a single electron occupying the metal–ligand antibonding $d_{x^2-y^2}$ orbital, but the additional d_{z^2} electron in nickel(I) decreases the effective nuclear charge and increases the radius of the ion. As in the case of high-spin nickel(II), the nickel(I) ion is larger than optimal for a porphyrin. The "compression" that would be experienced by a nickel(I) ion in a porphyrin environment would greatly destabilize the antibonding $d_{x^2-y^2}$ orbital. In all likelihood, it would be higher in energy than the porphyrin π^* orbital. Hydroporphyrins, on the other hand, have inherently larger hole sizes than porphyrins.[6–8a,9] OEiBC has been reported to accommodate high-spin nickel(II).[9]

Ample precedent can be found in the chemistry of nickel macrocycles for a correlation of hole size with ligand field strength,[69,70] the reduction potential of nickel,[14,71,72] and ultimately the energy of the $d_{x^2-y^2}$ orbital. N-methylated nickel cyclam macrocycles provide a good example. As the number of methyl groups on secondary nitrogens was increased from 0 to 4, the ligand field decreased,[70] and the potential of the nickel(II)/nickel(I) couple shifted 350 mV anodic.[72] The opposite trend might have been expected, given the inherent greater basicity of tertiary versus secondary amine donor ligands.[73] However, X-ray structural evidence established that the nickel–nitrogen distances increased upon methylation.[72,74] The increased hole size minimized unfavorable steric interactions within the macrocycle.

The reduction potential of the Ni^{II}(OEiBC)/Ni^{I}(OEiBC)$^-$

(61) Label in idealized D_{4h} symmetry.

(62) Stolzenberg, A. M.; Strauss, S. H.; Holm, R. H. *J. Am. Chem. Soc.* **1981**, *103*, 4763.
(63) (a) Strauss, S. H.; Pawlik, M. J. *Inorg. Chem.* **1986**, *25*, 1921. (b) Strauss, S. H.; Pawlik, M. J.; Skowyra, J.; Kennedy, J. R.; Anderson, O. P.; Spartalian, K.; Dye, J. L. *Inorg. Chem.* **1987**, *26*, 724. (c) Strauss, S. H.; Long, K. M.; Magerstädt, M.; Gansow, O. A. *Inorg. Chem.* **1987**, *26*, 1185.
(64) Stolzenberg, A. M.; Spreer, L. O.; Holm, R. H. *J. Chem. Soc., Chem. Commun.* **1979**, 1077.
(65) (a) Richardson, P. F.; Chang, C. K.; Hanson, L. K.; Spaulding, L. D.; Fajer, J. *J. Phys. Chem.* **1979**, *83*, 3420. (b) Chang, C. K.; Fajer, J. *J. Am. Chem. Soc.* **1980**, *102*, 848. (c) Chang, C. K.; Hanson, L. K.; Richardson, P. F.; Young, R.; Fajer, J. *Proc. Natl. Acad. Sci. U.S.A.* **1981**, *78*, 2652.
(66) Fujita, E.; Fajer, J. *J. Am. Chem. Soc.* **1983**, *105*, 6743.
(67) Strauss, S. H.; Holm, R. H. *Inorg. Chem.* **1982**, *21*, 863.
(68) (a) Hoard, J. L. *Science* (Washington, D. C.) **1971**, *174*, 1295. (b) Hoard, J. L. *Ann. N.Y. Acad. Sci.* **1973**, *206*, 18.
(69) (a) Martin, L. Y.; DeHayes, L. J.; Zompa, L. J.; Busch, D. H. *J. Am. Chem. Soc.* **1974**, *96*, 4046. (b) Martin, L. Y.; Sperati, C. R.; Busch, D. H. *J. Am. Chem. Soc.* **1977**, *99*, 2968.
(70) Wagner, F.; Barefield, E. K. *Inorg. Chem.* **1976**, *15*, 408.
(71) Jubran, N.; Cohen, H.; Meyerstein, D. *Isr. J. Chem.* **1985**, *25*, 118.
(72) Barefield, E. K.; Freeman, G. M.; Van Derveer, D. G. *Inorg. Chem.* **1986**, *25*, 552.
(73) Arnett, E. M. *Acc. Chem. Res.* **1973**, *6*, 404.
(74) Bosnich, B.; Mason, R.; Pauling, P. T.; Robertson, G. B.; Tobe, M. L. *Chem. Commun.* **1965**, 97.

couple is considerably negative of those for the corresponding couple in F_{430}[20,75] and in many tetraazamacrocyclic complexes.[14,16,72,76] Thus, it is possible that the hole size of OEiBC may be smaller than optimal for nickel(I).

A Biologically Significant Difference between Classes of Tetrapyrrole Macrocycles. We have seen that the metal-to-nitrogen distance in the planar porphyrin of minimal strain is considerably larger than optimal for low-spin nickel(II). Actual structures of nickel(II) porphyrins are planar or somewhat distorted and have average Ni–N distances of about 1.97 Å.[9,68] Any distortion that could further improve the Ni–N interaction must not be sufficiently exergonic to offset the expense of decreasing the π overlap in the porphyrin.

The extensive X-ray structural results of Ibers, Eschenmoser, and Kratky demonstrate that the increased flexibility (decreased aromaticity) of nickel hydroporphyrin complexes permits them to adopt markedly saddle-shaped (S_4-ruffled) structures.[5-9] This distortion entails twisting the two transannular five-membered rings in opposite directions about the N–Ni–N axis contained by these rings. Meso carbons are alternately above and below the plane containing nickel and the four nitrogen atoms. Ruffling stabilizes low-spin nickel(II) by reducing Ni–N distances.[6-9,68] The steepness of the saddle has been demonstrated to increase with the extent of saturation of the hydroporphyrin macrocycle π-system.[8a,9,11] Since the inherent hole size of a planar hydroporphyrin macrocycle increases with the saturation level, more saturated macrocycles must ruffle to a greater degree to achieve the Ni–N distance that is typical for low spin nickel(II) in these compounds (about 1.92 Å or less).[9]

Our results establish that it is precisely the more saturated and therefore more ruffled hydroporphyrin macrocycles that can accommodate a large nickel(I) ion. This ion probably has an optimal Ni–N distance in excess of 2.1 Å.[77] It is truly remarkable that the OEiBC macrocycle can expand and contract its core over a range of nearly 0.4 Å to provide near-optimal bond lengths for both members of the Ni(II)/Ni(I) couple. Clearly, the hole sizes/ligand field strengths of hydroporphyrin macrocycles can be varied over a wide range at little cost in energy. The large range of variation stretches the concept of hole size/ligand field strength to the limits of usefulness for these ligands. The hole size/ligand field strength is no longer a property defined for the macrocycle but rather is defined for the macrocycle within a specific complex. The more rigid porphyrin macrocycles, on the other hand, enforce a narrow range of Ni–N distances/ligand field strengths. The distances enforced are nonoptimal for either low-spin or high-spin nickel(II).

It is instructive to recast this point in more abstract terms. The energy of a macrocyclic ligand as a function of atomic coordinates (conformational energy) is described by an *n*-dimensional surface. We have just shown that the gradient of this surface along the coordinates that relate to the center-nitrogen distance is less for hydroporphyrins than for porphyrins. The shallowness of the conformational energy surface along this and other coordinates is what is really implied by "increased flexibility".

Conformational energy surfaces can also be defined for corrins, oxoporphyrins, and other tetrapyrroles. These surfaces will have distinct global energy minima and gradients. The energy surface for corrins, which lack one meso carbon, would be expected to have a minimum at small center-nitrogen distances. On the basis of the structure of one nickel oxoporphyrin complex,[29] the energy surface for oxoporphyrins might be expected to have a minimum at relatively large center-nitrogen distance and a steeper gradient than the hydroporphyrin surface.

Figure 5 is an "artist's conception" of projections of the different hypothetical energy surfaces on the energy versus center-nitrogen distance plane. (It is not to be taken literally. The energy scale

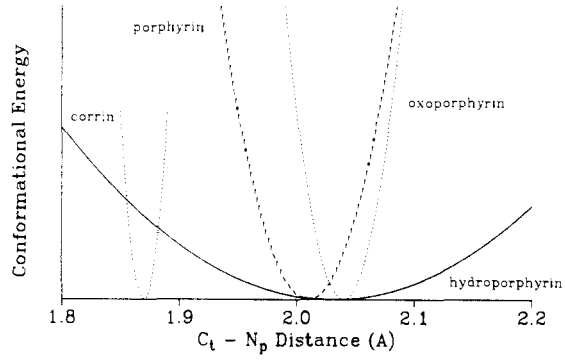

Figure 5. Projections of hypothetical *N*-dimensional conformational energy surfaces of several classes of tetrapyrrole macrocycles onto the energy, center-nitrogen distance plane. This figure is intended to illustrate that the conformational energy minima of different macrocycles occur at different center-nitrogen distances and that the gradients of the energy with respect to this parameter vary with macrocycle. See text.

and curve shapes are arbitrary and are not intended to convey actual physical quantities. C_t–N distances of minima are approximate.) Though a gross simplification, Figure 5 helps to clarify the concepts under discussion and graphically illustrates an important hypothesis that we advance here. *A fundamental difference (if not the fundamental difference) between porphyrins, hydroporphyrins, corrins, oxoporphyrins, and other tetrapyrrole macrocycles is their optimal hole size and the range of hole sizes that are readily accessible in their complexes.* Apparently, nature has devised several families of tetrapyrroles that are fine tuned differently. The tetrapyrrole best suited for a particular biological function depends upon the metal ion radii required during the process. For example, F_{430}-dependent methanogenesis involves both nickel(II) and nickel(I) oxidation states. Corrins would be rather poorly suited for this task since they would severely destabilize the nickel(I) oxidation state. Hydroporphyrins can readily accommodate both oxidation states of nickel and are therefore clearly best suited for use in nickel-dependent methanogenesis.

Figure 5 also clarifies the meaning of "accommodate" in this discussion. We do not mean to imply that porphyrins are incapable of coordinating large metal ions. The existence of $Sn(TPP)Cl_2$ and $Sn(OEP)Cl_2$ demonstrates that they can. In these complexes Sn is centered in the porphyrin plane, and the average Sn–N distance is 2.099 (2)[78] and 2.082 (2),[79] respectively. Expansion of the porphyrin core to this size comes at the cost of a substantial increase in the conformational energy of the porphyrin. Coordination of the strongly complexing tin(IV) ion is sufficiently exergonic to compensate for the endergonicity of the conformational changes. Even so, the Sn–N bond lengths in these complexes are about 0.05 Å shorter than the preferred value for Sn with monodentate nitrogen ligands.[68] Core expansion (or contraction for that matter) will not occur if the other changes coupled to the conformational change are not sufficiently exergonic.

The Relationships of Substituent Stereochemistry, Macrocycle Flexibility, and Axial Ligation Equilibria ("Axial Electrophilicity"). The discussion began with the factors affecting the electronic energies of complexes and has progressed to the conformational energies of the complexes. Electronic energies generally are large and dominate the choice of the ground state. However, when the difference in the electronic energies of various states is small, conformational energies can play a major role in defining the relative stability of these states. Thus, the understanding of tetrapyrrole conformational energies that we have developed here permits us to rationalize several aspects of tetrapyrrole chemistry.

Eschenmoser, Kratky, and co-workers analyzed the X-ray structures of an extensive series of free-base and nickel(II) octaethylhydroporphyrins.[9,80] The overall conformation of the

(75) Kratky, C.; Fässler, A.; Pfaltz, A.; Kräutler, B.; Jaun, B.; Eschenmoser, A. *J. Chem. Soc., Chem. Commun.* **1984**, *1368*.
(76) Rillema, D. P.; Endicott, J. F.; Papaconstantinou, E. *Inorg. Chem.* **1971**, *10*, 1739.
(77) X-ray studies will be necessary to determine the coordination geometry and bond lengths actually associated with nickel(I) in these complexes.
(78) Meyer, E. F., Jr. *Acta Crystallogr. Sect. B: Struct. Crystallogr. Cryst. Chem.* **1972**, *28B*, 2162.
(79) Cullen, D. L.; Meyer, E. F., Jr. *Acta Crystallogr. Sect. B: Struct. Crystallogr. Cryst. Chem.* **1973**, *29B*, 2507.

macrocycle (planar versus ruffled) was correlated with the spatial disposition of the pyrroline rings and attached ethyl substituents. Free-base complexes were essentially planar. The pyrroline rings of these complexes adopted shallow half-chair conformations with pseudoequatorial ethyl groups. Nickel complexes were ruffled for the reasons discussed above. Individual pyrroline rings adopted half-chair conformations but were not conformationally independent. These rings coupled to give two so called W-shaped conformations (viewed in cylindrical projection) in which the C_β–C_β bonds paralleled the inclination of the macrocycle saddle. The two W conformations were related by inversion of the sense of the ruffle (two enantiomerically related senses exist) and inversion of all half-chairs. The preferred W conformation appeared to maximize the number of pseudoaxial ethyl groups. It was considered truly remarkable that the contraction of the macrocycle core induced by the small nickel ion caused ruffling of the macrocycle, which in turn determined the conformation of the pyrroline rings, and thereby defined the preferred stereochemistries of the substituents at the ligand periphery.[80]

We recently demonstrated the applicability of the structural results to nickel hydroporphyrin complexes in solution.[5] A substantial body of evidence was consistent with ruffled conformations for *cis*- and *trans*-Ni(OEC) in solution. β-Proton coupling constants established that the pyrroline ring ethyl groups of *trans*-H_2(OEC) and *trans*-Ni(OEC) adopted conformations similar to those seen in the X-ray structures. The pyrroline ring conformation of *cis*-H_2(OEC) permitted the *cis*-ethyl substituents to move away from each other. The enhanced Ni–N interactions in the ruffled *cis*-Ni(OEC) complex were sufficiently exergonic that the *cis*-ethyl groups became reeclipsed. Interestingly, the barrier to inversion of the sense of ruffling was smaller for *cis*-Ni(OEC) than for *trans*-Ni(OEC). The unfavorable interactions of the *cis*-ethyl groups increased the energy of the ruffled conformation of the macrocycle and thereby decreased the exergonicity of the ruffling process. Clearly, substituents interactions are important to the conformational energy of tetrapyrrole complexes. Further consideration of this point suggests that the important chain of cause and effect may not run from nickel outward to the substituents but from the substituents inward to modulate the coordination environment at nickel.

Why might it be desirable to modulate the environment at nickel with peripheral substituents? It is because "flexibility" is not always a virtue. Flexibility could potentially lock a complex into a single conformation or oxidation state. Consider the reaction of a low-spin nickel(II) complex with added ligand. Ligand binding occurs only if the free energy of the five- or six-coordinate complex is less than that of the square-planar complex. The lone pair on the ligand interacts with the d_{z^2} orbital, which is metal–ligand antibonding in the low-spin square-planar complex. There is no net bonding since both orbitals are filled. However, a sufficiently strong field ligand will decrease the energy difference between the d_{z^2} orbital and the empty $d_{x^2-y^2}$ orbital until it is less than the pairing energy. An electron enters the metal–ligand (macrocycle) antibonding $d_{x^2-y^2}$ orbital, yielding a high-spin complex. The net interaction of the axial ligand lone pair and the d_{z^2} orbital becomes bonding. The electron in the $d_{x^2-y^2}$ orbital greatly increases the effective radius of the nickel ion. As in the case of nickel(I), the energy of the $d_{x^2-y^2}$ orbital will be too high for these changes to occur, unless the core of the macrocycle can expand. The increase in conformational energy upon core expansion must be offset by the exergonicity of the new nickel–ligand bond(s). The macrocycles capable of readily expanding their core to accommodate the large nickel(I) ion are those that can ruffle to contract the core for the small low-spin nickel(II) ion.[9] However, the exergonic free energy change associated with ruffling becomes an endergonic contribution to the conformational energy for ligand binding because the macrocycle must flatten and expand in the process. Certain substituent stereochemistries decrease the exergonicity and extent of ruffling in the low-spin complexes. In turn, high-spin nickel(II) will be more accessible, and ligand affinities should be higher for these complexes. Note that native F_{430}, which is not the thermodynamically preferred epimer of F_{430} and therefore ruffles less deeply, has a greater affinity for axial ligands than the stable epimer.[4c] An analogous argument can be presented to show that increased stability of the low-spin nickel(II) complex can limit the stability of the nickel(I) oxidation state. Similarly, unfavorable substituent stereochemistries in the core expanded conformations can have the same effect.

Eschenmoser's group observed that the tendency to bind axial ligands or the so called "axial electrophilicity" of nickel(II) tetrapyrroles increases in the series corrin $\ll$ porphyrin < chlorin < isobacteriochlorin < bacteriochlorin < pyrrocorphin.[9] The order correlates with the deviation from planarity of the macrocycle in the square-planar complex. This was rationalized by suggesting that the tendency of the nickel ion to reach "saturation of its electrophilicity in the equatorial plane" was offset by the strain induced by ruffling the macrocycle, leaving nickel with residual electrophilicity in these complexes.[80] The macrocycle is planar in six-coordinate hydroporphyrin complexes and has Ni–N distances of 2.09 Å.[75] (The shorter, 2.04 Å axial Ni–N bond is noteworthy.) The release of strain when the macrocycle flattened upon axial coordination was suggested to contribute to the high electrophilicity of nickel in the ruffled hydroporphyrin complexes.

Our previous discussion shows that the "axial electrophilicity" model is incomplete. It ignores the details and effects of the spin state equilibrium, the importance of the dramatic increase in the radius of nickel(II) in the equatorial plane that results, and the expansion of the macrocycle core that is required to accommodate high-spin nickel(II). The model is also inaccurate. A large buildup of strain will limit both the contraction of the macrocycle core and the steepness of the macrocycle ruffling. Therefore, one would expect that nickel porphyrin, which has the longest Ni–N bonds, should have the largest residual electrophilicity and the greatest affinity for axial ligands. This is not the case. Nickel porphyrins complexes with bound axial ligands are only observed in the solid state[81] or under forcing conditions such as with use of neat ligand (pyridine) for the solvent.[82] The release of strain on flattening a ruffled macrocycle does play a role in ligand binding equilibria. It decreases the endergonic contribution to the free energy that is associated with flattening the macrocycle.

Phlorin Formation. The ideas presented above help rationalize the disproportionation to phlorins that was observed in certain cases. Several of the nickel(I) complexes may have conformational energies (OEC) or unfavorable interactions between substituents (DMOEiBC) that lessen their thermodynamic stability. Although phlorins have not been structurally characterized, the somewhat analogous porphodimethene complex Ni(OEPMe$_2$), which has two nonadjacent saturated meso positions (see drawing), is markedly S_4 ruffled and has rather short Ni(II)–N bonds (1.908 (5) Å).[83] The saturation of one meso position in the phlorins introduces a permanent kink in the planarity of the macrocycle and might be expected to induce conformations with short Ni–N bonds. Both the enhanced stability of low-spin nickel(II) and the creation of a new C–H bond contribute to the thermodynamic stability of phlorins relative to nickel(I).

Implications for Models of F_{430}. We have stated that Ni(OEiBC) shows promise as a model for the reactivity of F_{430}. The spectroscopic and structural features of Ni(OEiBC) are quite different than those of F_{430}. Regardless of its spectroscopic and structural failings, Ni(OEiBC) provides the best and only tetrapyrrole model for F_{430} that is currently available. With the exception of F_{430} itself, Ni(OEiBC) is the only tetrapyrrole to date

(80) Eschenmoser, A. *Ann. N. Y. Acad. Sci.* **1986**, *471*, 108.

(81) Kirner, J. F.; Garofalo, J., Jr.; Scheidt, W. R. *Inorg. Nucl. Chem. Lett.* **1975**, 107.

(82) (a) Baker, E. W.; Brookhart, M. S.; Corwin, A. H. *J. Am. Chem. Soc.* **1964**, *86*, 4587. (b) McLees, B. D.; Caughey, W. S. *Biochemistry* **1968**, *7*, 642. (c) Abraham, R. J.; Swinton, P. F. *J. Chem. Soc. B* **1969**, 903. (d) Cole, S. J.; Curthoys, G. C.; Magnusson, E. A.; Phillips, J. N. *Inorg. Chem.* **1972**, *11*, 1024. (e) Pasternack, R. F.; Spiro, E. G.; Teach, M. *J. Inorg. Nucl. Chem.* **1974**, *36*, 599. (f) Walker, F. A.; Hui, E.; Walker, J. M. *J. Am. Chem. Soc.* **1975**, *97*, 2390.

(83) Dwyer, P. N.; Buchler, J. W.; Scheidt, W. R. *J. Am. Chem. Soc.* **1974**, *96*, 2789.

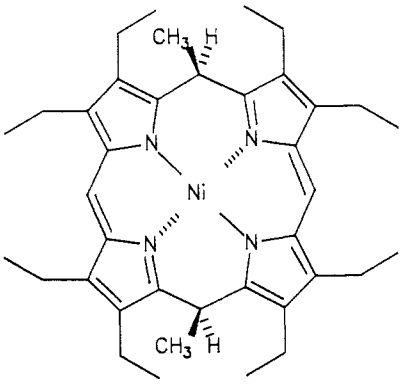

Ni(OEPMe$_2$)

that can be reduced quantitatively to an isolable nickel(I) complex. We report elsewhere that Ni^{I}(OEiBC)$^-$ is an extremely reactive nucleophile.[27] It does not react by a radical mechanism, unlike other nickel(I) complexes.[39,40] Further investigation of F_{430} and F_{430}-containing enzymes will be necessary to determine whether our results are relevant to its chemistry.

Would more extensively saturated nickel hydroporphyrins (i.e., hexahydroporphyrins or higher) provide better models? Possibly not. Spectroscopic and structural details of these complexes may more closely resemble those of F_{430}, but it is conceivable that some if not all nickel hexahydroporphyrin complexes will afford nickel(II) anion radical rather than nickel(I) complexes upon reduction. Extrapolations of certain results might suggest that more extensive saturation of the macrocycle π-system should favor nickel(I) by increasing macrocycle flexibility, increasing macrocycle hole size ($d_{x^2-y^2}$ less destabilized), and raising the energy of the macrocycle π^* orbital. On the other hand, our results show that the differences in the free energies of the nickel(I), nickel(II) anion radical, and phlorin forms of a specific complex are relatively small. The ground state of reduced complexes is determined by a delicate balance of interrelated electronic, conformational, and substituent effects. Nickel(I) could be inaccessible if the ruffling that stabilizes low-spin nickel(II) in the macrocycle is sufficiently exoergic or core expansion sufficiently endoergic.

Summary. The principal experimental results of this investigation of the reductions of nickel porphyrin and hydroporphyrin complexes are listed below.

(1) Ni^{I}(OEiBC)$^-$ results upon chemical or electrochemical reduction of Ni(OEiBC).

(2) Reduction of Ni(OEC) and Ni(DMOEiBC) affords unstable nickel(I) complexes which are further reduced or disproportionate. The chlorin–phlorin anion Ni(OECH)$^-$ is the stable product of the reduction of Ni(OEC).

(3) Reduction of Ni(OEP) yields an unstable nickel(II) anion radical Ni(OEP)$^{\bullet-}$ which undergoes further reduction or disproportionation to afford the stable phlorin anion complex Ni(OEPH)$^-$.

(4) The chemical reductions of Ni(TPP), Ni(TPC), and Ni(TPiBC) produce mixtures of anion radical, phlorin anion, and phlorin dianion radical species.

Our results, when considered in light of the results of investigations of the structures and conformations of nickel(II) hydroporphyrins, lead to the following conclusions.

(1) Significant and potentially biologically relevant changes in metal-based reactivity occur upon substitution of one class of tetrapyrrole macrocycle for another.

(2) The site of reduction depends both upon the relative energies of the macrocycle E_g π^* orbital and the nickel $d_{x^2-y^2}$ orbital.

(3) The energy of the macrocycle π^* orbital depends upon the saturation level of the macrocycle. The higher energy of this orbital in the isobacteriochlorin macrocycle favors reduction of the nickel ion.

(4) The energy of the metal $d_{x^2-y^2}$ orbital depends upon the hole size/ligand field strength of the macrocycle.

(5) The reduction of Ni(OEP) to Ni(OEP)$^{\bullet-}$ and of Ni(OEC) to Ni^{I}(OEC)$^-$, despite the fact that their π^* orbitals are at nearly the same energy, leads to the conclusion that *hydroporphyrins and porphyrins produce different ligand fields* for a coordinated nickel ion.

(6) The macrocycles that best accommodate the large 2.1 Å Ni–N distance required for nickel(I) are precisely those than can ruffle to decrease their core size to accommodate low-spin nickel(II) with Ni–N distances of 1.92 Å.

(7) The hole size/ligand field strengths of hydroporphyrins can be varied over a wide range at little cost in energy—i.e., hole size is not well defined for hydroporphyrin macrocycles.

Finally, we advance two new hypotheses.

(1) A fundamental difference (if not the fundamental difference) between porphyrins, hydroporphyrins, corrins, oxoporphyrins, and tetrapyrrole macrocycles is their optimal hole size and range of hole sizes that are readily accessible in their complexes. Stated in other words, the conformational energy surfaces of these macrocycles are decidedly different.

(2) The stereochemistry of substituents on the periphery of a tetrapyrrole macrocycle affects the conformation energy surface of the macrocycle. Thus, substituents can modulate the site of reduction and ligand-binding equilibria of the coordinated metal ion.

Acknowledgment. We thank Professor William H. Orme-Johnson, Dr. Leonard Schussel, and Neil Bastian for assistance in obtaining EPR spectra. This work was supported by the Camille and Henry Dreyfus Foundation (Young Faculty Grant to A.M.S.), the Research Corporation, and the National Institutes of Health (GM33882).